### Title

Global warming and the hydrologic cycle




### Journal

Journal of Hydrology, 174(1-2)

### ISSN

0022-1694



### Authors

Loaiciga, Hugo A

Valdes, Juan B

Vogel, Richard

et al.



### Publication Date

1996

### DOI

10.1016/0022-1694(95)02753-x

Peer reviewed

ELSEVIER

Journal of Hydrology 174 (1996) 83–127

Journal of Hydrology

# Global warming and the hydrologic cycle

Hugo A. Loaiciga[a,*], Juan B. Valdes[b], Richard Vogel[c], Jeff Garvey[d], Harry Schwarz[e]

[a]*Department of Geography and Environmental Studies Program, University of California, Santa Barbara, CA 93106-4060, USA*

[b]*Department of Civil Engineering and Climate System Research Program, Texas A & M University, College Station, TX 77843, USA*

[c]*Department of Civil Engineering, Tufts University, Medford, MA 02155, USA*

[d]*Boyle Engineering Corporation, San Diego, CA 92111, USA*

[e]*Department of Geography, Clark University, Worcester, MA 01609, USA*

Received 30 August 1994; revision accepted 17 March 1995

**Abstract**

Starting with a review of the basic processes that govern greenhouse warming, we have demonstrated that the hydrologic cycle plays a key role in the heat balance of the Earth's surface–atmosphere system. Through the water and other climatic feedbacks, the hydrologic cycle is shown to be a key factor in the climate's evolution as greenhouse gases continue to build up in the atmosphere. This paper examines the current predictive capability of general circulation models linked with macroscale and landscape-scale hydrologic models that simulate regional and local hydrologic regimes under global warming scenarios. Issues concerning hydrologic model calibration and validation in the context of climate change are addressed herein. It is shown that the natural uncertainty in hydrologic regimes in the present climate introduces a signal-to-noise interpretation problem for discerning greenhouse-induced variations in regional hydrologic regimes. Simulations of river basins by means of macroscale hydrologic models nested within general circulation models have been implemented in a few selected cases. From the perspective of water resources management, such simulations, carried out in detail under greenhouse-warming scenarios in midlatitudinal basins of the United States, predict shorter winter seasons, larger winter floods, drier and more frequent summer weather, and overall enhanced and protracted hydrologic variability.

All these predictions point to potentially worsening conditions for flood control, water storage, and water supply in areas of semiarid midlatitudinal climates currently dependent of spring snowmelt. Little information of this type is currently available for other areas of the world. Practice of sound water resources engineering principles ought to be adequate to cope with additional hydrologic uncertainty that might arise from global warming.

* Corresponding author.


*SSDI* 0022-1694(95)02753-X

## 1. Introduction

The rapid build up of greenhouse gases in the post-Industrial Revolution era has given rise to one of the greatest scientific puzzles in the history of science. Will the Earth's surface and the lower part of the atmosphere warm up owing to increased concentrations of carbon dioxide ($CO_2$), methane ($CH_4$), ozone ($O_3$), nitrous oxide ($N_2O$), chlorofluorocarbons (CFCs), and other greenhouse gases? If so, how much will the increase in average temperature be? More importantly, what will the consequences of a higher surface temperature on the Earth's climate, humans, and the environment at large be?

Scientists are tackling these complex questions, resulting in a frenzy of activity mostly concentrated on the potential evolution of the Earth's climate and the measurement of important factors that regulate the global climate (solar irradiance, surface albedo, surface energy fluxes, cloud properties, surface temperature, and greenhouse-gas concentrations, among others).

In the United States, these research efforts are coordinated through the United States Global Change Research Program (USGCRP), and funded through appropriations to a variety of agencies such as the National Science Foundation (NSF), the National Atmospheric and Space Administration (NASA), the National Oceanic and Atmospheric Organization (NOAA), the Environmental Protection Agency (EPA), the United States Geological Survey (USGS), and the Department of Energy (DOE) (see Goodwin, 1994).

In the international arena, a variety of research projects and observational studies have been launched concerning the global climate system, the hydrologic cycle, atmospheric gases and chemistry, energy budgets and radiation fluxes, ocean circulation and coupling with the atmosphere, and ecosystems, at a variety of spatial and temporal scales. Examples of some of the best known observational studies and research programs are (several of these are interdependent): the World Climate Research Programme (WCRP), the International Geosphere–Biosphere Programme (IGBP), the Global Energy and Water Cycle Experiment (GEWEX), the International Satellite Land Surface Climatology Project (ISLSCP), the Global Precipitation Climatology Project (GPCP), the Tropical Rainfall Measuring Mission (TRMM), the Earth Radiation Budget Experiment (ERBE), the Tropical Ocean Global Atmosphere (TOGA) project, the World Ocean Circulation Experiment (WOCE), the International Satellite Cloud Climatology Project (ISCCP), the Hydrologic Atmospheric Pilot Experiment (HAPEX), the Sahelian Energy Budget Experiment (SEBEX); the Terrestrial Initiative in Global Environmental Research (TIGER), the Amazon Region Micrometeorological Experiment (ARME), the Atmospheric Radiation Measurement (ARM) program, the Joint Global Ocean Flux Study (JGOFS); the International Global Atmospheric Chemistry (IGAC) project; Past Global Changes (PAGES) program; the Boral Forest Study (BOREAS), and the mammoth Earth Observing System (EOS), centerpiece of NASA's Mission to Planet Earth, which is a pivotal element of the US Global Change Research Program.

Fig. 1 provides the locations of various hydroclimatic observational studies.

The global climate system and its evolution as a result of increased concentration in

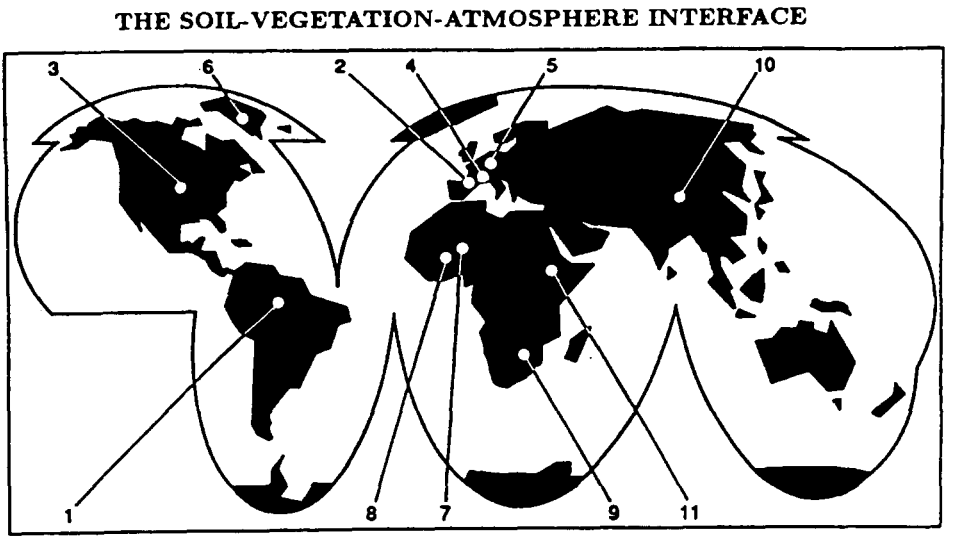


Fig. 1. Location of study sites for regional climate and hydrology (1, ARME; 2, HAPEX (MOBILHY); 3, First ISLSCP Field Experiment (FIFE); 4, ISLSCP (La Crau); 5, ISLSCP (LOTREX-HIBE88); 6, ISLSCP (Greenland); 7, ISLSCP (Niger); 8, SEBEX; 9, ISLSCP (Botswana); 10, HAPEX (Heihe river); 11, ISLSCP (Sudan); adapted from Shuttleworth, 1993).

greenhouse gases are complex and poorly understood phenomena. How do global climate processes, such as those leading to higher surface temperature, affect regional and local hydrologic regimes?. For hydrologic design and water resources planning, the answers are vital.

In this paper, we review the issues involved, and state-of-the-art knowledge of global warming and the hydrologic cycle. The controversy about anthropogenic greenhouse warming effects on the global and regional hydrologic cycles will not be resolved shortly, if ever. But some key issues on how greenhouse warming is likely to impact the global circulation of water vapor are now reasonably well settled.

The objective of the Task Committee on Global Warming and Hydrologic Variability of the American Society of Civil Engineers, under whose aegis this work was conducted, was to assess the status of knowledge on induced greenhouse warming and its impact on the global and regional hydrologic cycles, as well as possible implications of greenhouse warming for water resources engineering. Our findings are presented in this paper.

## 2. A few facts on anthropogenically induced greenhouse warming

### *2.1. The greenhouse effect*

The key to understanding how the Earth's atmosphere regulates surface temperature resides in the so-called greenhouse effect. Fig. 2 is a simplified illustration of the

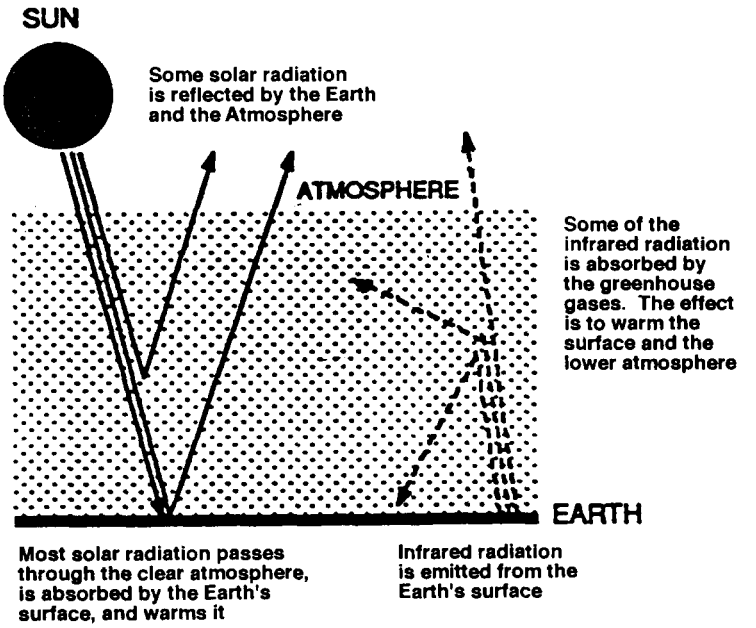


Fig. 2. Basic elements of the atmospheric greenhouse effect (from IPCC, 1990. Reprinted by permission of Cambridge University Press.)

greenhouse effect. Solar irradiance, the solar power per unit area intercepted at the mean Earth–Sun distance, is the major source of energy that heats the Earth. It has been measured recently via satellites to range between 1365 and 1372 W $m^2$ (watts per square meter, Ramanathan et al., 1989a). Because the Earth's atmosphere has a spherical shape, the average flux of solar radiation at the top of the atmosphere (about 100 km above the Earth's surface) per square meter of the Earth's surface — this is called the solar insolation — is approximately 342 W $m^{-2}$, or one fourth of the solar irradiance. The one fourth factor is equal to the ratio of the area of the Earth's disc ($\pi R^2$, where $R$ is the Earth' radius) to the Earth's surface area ($4\pi R^2$) (see Monteith, 1973). Most of the solar radiation reaching the Earth is in the wavelength range of 0.15–3.0 $\mu$m (micrometers), with maximum intensity at about 0.5 $\mu$m. Radiation in this wavelength range is called shortwave radiation and it contains the ultraviolet, visible (0.4–0.76 $\mu$m), and near-infrared regions of the electromagnetic spectrum (Mitchell, 1989).

Of the 342 W $m^{-2}$ at the top of the atmosphere, approximately 169 W $m^{-2}$ (mostly in the visible range of the electromagnetic spectrum) are absorbed by the Earth's surface. This absorbed radiative flux warms the surface of the Earth. About 68 W $m^{-2}$ of the incoming solar insolation are absorbed by the atmosphere contributing directly to its heating. The remainder of the solar insolation, or 105 W $m^{-2}$, is reflected back to outer space, and, thus, the net input of solar radiation to the surface–atmosphere system is $342 - 105 = 237$ W $m^{-2}$.

In the absence of long-term net gains or losses of energy, the surface–atmosphere

system can be assumed to emit radiative energy as a blackbody with an equivalent mean effective radiative temperature of approximately −18°C. The atmosphere is generally cooler than the Earth's surface, however, the latter having a global mean value of approximately 15°C. The difference between the mean effective radiative temperature of the surface–atmosphere system (−18°C) and the Earth's mean surface temperature (15°C), or 33°C, is due to the greenhouse effect of the atmosphere (Ramanathan et al., 1989).

The greenhouse effect takes place as the Earth's surface is warmed up by absorbed solar radiation. The Earth's surface emits radiant energy approximately like a blackbody, with most of the outgoing radiation being between 4.0 and 60 $\mu$m, or in the so-called infrared (or long-wave) range of the electromagnetic spectrum.

The atmosphere is generally cooler than the Earth's surface, as we have seen. Therefore, gas molecules in the atmosphere will absorb more energy than they emit, as required by the blackbody radiation law (Stefan–Boltzmann law). The net result of these emission and absorption processes in the surface–atmosphere system is that part of the infrared radiation emitted from the Earth's surface is trapped by atmospheric gases, giving rise to the greenhouse effect. This entrapment of infrared radiation (estimated at 153 W $m^{-2}$ under current 'equilibrium' conditions) contributes to atmospheric warming and to infrared emissions from the atmosphere back to the Earth 's surface. The 'greenhouse-warmed' atmosphere also emits infrared radiation to outer space. The Earth's surface–atmosphere system eventually reaches a state of radiative equilibrium whereby the 'blackbody cooling' from infrared radiative emissions to outer space (237 W $m^{-2}$) balance the net energy input from the sun (237 W $m^{-2}$, which equals the solar insolation of 342 W $m^{-2}$ minus 105 W $m^{-2}$ reflected back to outer space by the atmosphere and the Earth's surface). Blackbody cooling emissions prevent a runaway heating of the Earth's surface owing to the greenhouse effect. In contrast, the planet Venus, whose atmosphere is over 90% (by volume) carbon dioxide, has an equilibrium surface temperature of about 477°C with an estimated greenhouse heating of 523°C, compared with a greenhouse heating on Earth of 33°C.

Radiative equilibrium conditions as they now exist on Earth have resulted in a global mean surface temperature of about 15°C. The equilibrium temperature profile from the Earth's surface to the top of the atmosphere, however, is rather complicated, showing pronounced temperature inversions in the middle and upper atmosphere (see Fig. 3). In the troposphere, the temperature profile is determined by radiative and convective (latent heat and turbulent heat fluxes) heat transfer. In the upper zones of the atmosphere, radiative heat balance determines the temperature profile.

Surprisingly, the greenhouse theory of climate change was already presented in 1896 by Arrhenius, apparently the first scientist to have investigated the effect of increased $CO_2$ on surface temperature. His estimates of surface temperature increases as a result of doubling atmospheric $CO_2$ are in rather good agreement with modern predictions by general circulation models to be discussed later. Arrhenius acknowledged in his 1896 study earlier contributions to the understanding of the greenhouse effect by the French mathematician Jean-Baptiste Fourier dating back to 1827 (see Ramanathan, 1988).

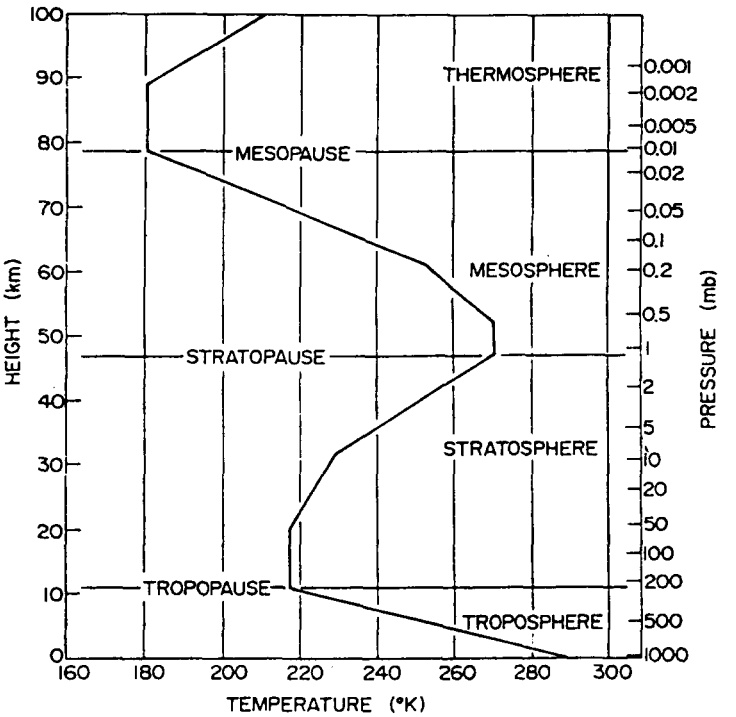


Fig. 3. Vertical atmospheric temperature profile. Degrees K is equal to °C + 273.15. (From Peixoto and Oort, 1992. Reprinted by permission of the American Institute of Physics.)

Table 1
Concentrations and residence times of important greenhouse gases.

| Characteristic | Greenhouse gas | | | | | | |
|---|---|---|---|---|---|---|---|
| | $H_2O$ | $CO_2$ | $CH_4$ | CFC-11 | CFC-12 | $N_2O$ | $O_3$ [a] |
| Concentration | ppmv | ppmv | ppmv | pptv | pptv | ppbv | ppbv |
| Preindustrial (1750–1800) | 3000 | 280 | 0.8 | 0 | 0 | 285 | 1–15[b] |
| 1990 | 3000 | 353 | 1.72 | 280 | 484 | 310 | 10–100 |
| Residence time | 10–15 days | 50–100 years | 10 years | 65 years | 130 years | 150 years | NA[c] |

Symbols: $H_2O$, water vapor; $CO_2$, carbon dioxide; $CH_4$, methane; CFC-11, $CFCl_3$; CFC-12, $CF_2Cl_2$; $N_2O$, nitrous oxide; $O_3$, ozone; ppmv, parts per million volume; ppbv, parts per billion volume; pptv, parts per trillion volume.

[a] Below 12 km.

[b] Estimated value.

[c] Ozone is continuously produced by photolisis in the stratosphere.

NA; not applicable.

### 2.2. Greenhouse gases and equilibrium conditions

The predominant greenhouse gases are water vapor and carbon dioxide. Together with cloud particles (water droplets, aerosols, and ice crystals), water vapor and carbon dioxide contribute to about 95% of the greenhouse effect. The other 5% is contributed mainly by ozone, methane, nitrous oxide, and, since their inception in the 20th century, by chlorofluorocarbons (CFCs). Table 1 (adapted from Ramanathan, 1988, and the Intergovernmental Panel on Climate Change, 1990) shows the concentrations of the main greenhouse gases since the Industrial Revolution (roughly, 1765, for England). All the gases in Table 1 absorb infrared radiation emitted by the Earth's surface and thus contribute to the greenhouse effect. Water vapor, the most abundant, is found predominantly in the troposphere. Carbon dioxide, which is relatively well mixed in the troposphere and stratosphere, has increased its concentration by almost 73 ppmvs (parts per million volume) since the late-1700s. It has been estimated by many authors that if 1990-level emissions of $CO_2$ to the atmosphere remain unabated, its concentration in the atmosphere could nearly double from the pre-Industrial level of 280 ppmv by the year 2100 or thereabouts. $CO_2$ is an important byproduct of human activities. It currently contributes approximately 50 W $m^{-2}$ of the total 153 W $m^{-2}$ of greenhouse heating (water vapor contributes approximately 100 W $m^{-2}$, Mitchell, 1989). Climate predictions for 'double $CO_2$' ($2 \times CO_2$) conditions have become standard.

Even though the other greenhouse gases shown in Table 1 have relatively low concentrations when compared with water vapor and carbon dioxide, and their contributions to current greenhouse heating are minor, their global warming potentials are considerable. For example, considering their absorption strength, atmospheric residence time (lifetime), molecular mass, and time period over which climate effects are of concern, Shine et al. (1990), estimate that the global warming potentials of $CH_4$, $N_2O$, CFC-11, and CFC-12 relative to that of $CO_2$ are 63, 270, 4500, and 7100 times, respectively, over a 20 year period. Therefore, equal incremental emissions of, say, $CO_2$ and CFC-12, are estimated to have disproportionally unequal greenhouse warming potentials (7100 times larger for the latter).

The interaction of ozone and CFCs is also important to note at this point. Ozone is found predominantly in the stratosphere (about 90% of atmospheric ozone occurs in the stratosphere). There, it is an effective absorber of incoming solar ultraviolet radiation. The heating caused by such absorption of solar radiation is enough to cause the temperature inversion in the stratosphere, as shown in Fig. 3. CFCs are known to deplete stratospheric ozone (see, e.g. Graedel and Crutzen, 1993, for a review of this subject), therefore contributing to surface warming as the flux of solar radiation reaching the Earth's surface increases. On the other hand, the depletion of stratospheric ozone reduces heating of the stratosphere thereby cooling it. Therefore, it is seen that the interaction of CFCs and ozone creates problems of a very different nature in the troposphere and stratosphere. In the troposphere, CFCs and ozone enhance the greenhouse effect. In the stratosphere, CFCs absorb infrared radiation also, but their depletion of ozone there causes warming in the lower troposphere and at the Earth's surface, while cooling the stratosphere.

The previous discussion on the greenhouse effect and greenhouse warming summarizes some basic facts concerning the warming potential of greenhouse gases, in particular, carbon dioxide. Here is where factual knowledge ends, and where prediction, assumptions, and disputed hypotheses on induced global warming begin. Basic climatic variables, such as mean global surface temperature and atmospheric temperature distributions, cannot, at present, be accurately (i.e. within $\pm 0.5°C$) predicted under the $2 \times CO_2$ scenario. Prediction of regional hydrologic variations is even less certain. Nevertheless, the study of induced greenhouse warming has had very positive effects on the science of hydrology. Basic aspects of the hydrologic cycle are now better understood as a result of theoretical and observational studies on the role of water vapor in greenhouse warming. Hydrology has emerged as a science of central significance in the investigation of induced global warming (Eagleson, 1991; National Research Council, 1991). The potential for global warming may lead to a re-examination of methods for the planning of water resources projects and related critical facilities. The likely increase of uncertainty in regional hydrologic regimes associated with potential climatic change justifies pondering the resilience and robustness of water infrastructure. The role of the hydrologic cycle in induced greenhouse warming is further analyzed next.

## 3. The hydrologic cycle in the climate change puzzle

Fig. 4 shows a one-dimensional (vertical) representation of the various water reservoirs and fluxes of water, as well as coupled systems (land–atmosphere, ocean–atmosphere, biosphere–atmosphere) in the global hydrologic cycle. One of the great difficulties in modelling potential climatic change has been the strong

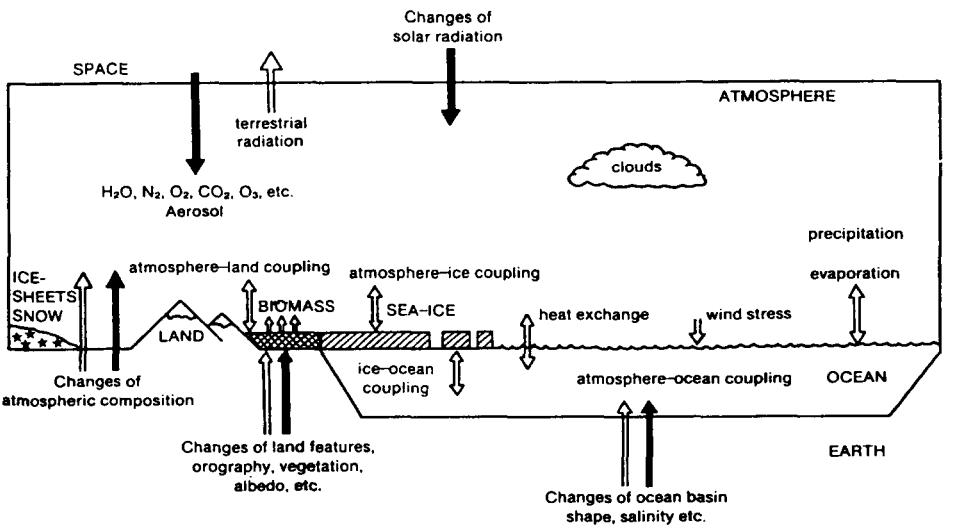


Fig. 4. A one-dimensional abstraction of the global hydrologic cycle (IPCC, 1990. Reprinted by permission of Cambridge University Press.)

influence that ocean–atmosphere coupling has on the transport of heat and atmospheric moisture around the globe. Potential modifications in the hydrologic cycle owing to induced global warming ultimately rest on coupled processes in the atmosphere, oceans, ice caps, land, and the biosphere. The study of the coupled nature of the climate system constitutes the global scale of the problem of greenhouse warming and hydrologic response to it. Fig. 5 provides a simplified representation of overriding factors that govern the global-scale coupling of climate (and climate change) and the hydrologic cycle. First, is the fact that the Earth is a rotating geoid, with its axis of rotation tilted relative to the Earth's revolution plane. This tilt, the Earth's sphericity, and the pattern of the Earth's revolution around the sun cause a seasonal and uneven latitudinal input of solar radiation, forcing heat transport from the warmer equatorial areas towards the poles. The Earth's rotation and the distribution of land areas and ocean areas determine the large-scale oceanic and atmospheric circulation patterns. These global-scale controlling factors of atmospheric heat balance and moisture circulation, coupled with continental-scale convective atmospheric transport caused by the uneven heat capacity of land masses (30% of the Earth's surface) and the oceans (70% of the Earth's surface) govern the convergence or divergence of atmospheric moisture in broad regions of the world. The Indian Ocean monsoons are a case in point.

Regional-scale hydrologic regimes, i.e. those at the scale of river basins, are determined by the large-scale climatic patterns of atmospheric circulation, latitude,

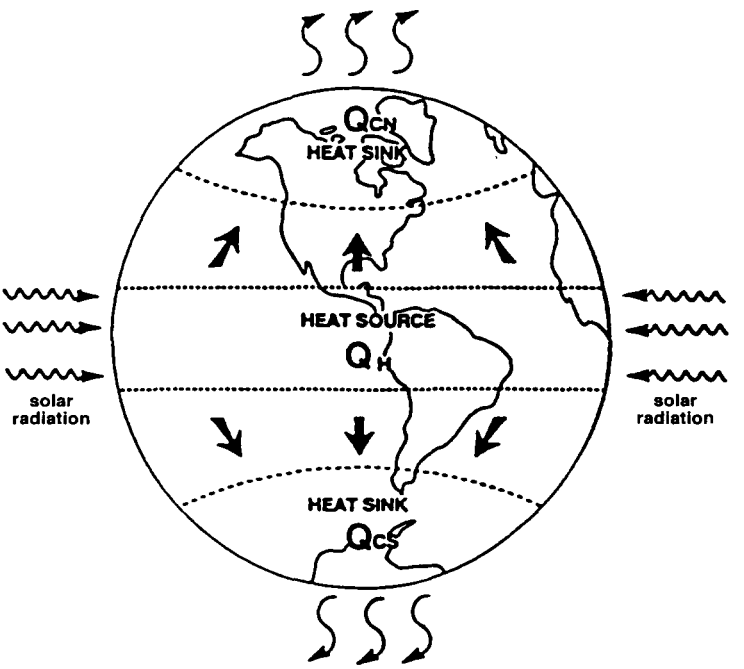


Fig. 5. Conceptual atmospheric heat engine (adapted from Lawford, 1993).

regional physiographic features, insularity, geology, vegetation, and land-use patterns. Let us examine in more detail possible connections between induced climate change and potential hydrologic cycle modifications at a global scale.

### 3.1. General Circulation Models (GCMs) and the hydrologic cycle

Various atmospheric GCMs are currently used to simulate climatic sensitivity to increased carbon dioxide concentrations and other important parameters. Some of the leading GCMs in common use today are: the Canadian Climate Center (CCC) model, the Geophysical Fluid Dynamic Laboratory (GFDL) model, the Goddard Institute for Space Studies (GISS) model, the National Center for Atmospheric Research (NCAR) model, the Oregon State University (OSU) model, and the United Kingdom Meteorological Office (UKMO) model (Cess et al., 1990). GCMs, of which the first account dates back to Phillips (1956), were initially developed to simulate average, synoptic-scale (i.e. $10^2$–$10^3$ km spatial scale), atmospheric circulation patterns for specified external forcing conditions. In this sense, they were originally conceived as boundary-value problem solvers, in contrast to the initial-value problem structure of numerical weather prediction models (dating back to Richardson, 1922), where atmospheric flow motion is computed starting from specified initial states. GCMs use the laws of conservation of mass (water vapor, air), momentum, and heat in the atmosphere, along with state-equations relating thermodynamic variables, expressed as coupled, non-linear, partial differential equations (Peixoto and Oort, 1992). These equations are discretized numerically and solved in a rotating system of coordinates in terms of atmospheric variables such as wind speed and direction, temperature, humidity, surface pressure, precipitation, etc. Multiple vertical layers are used to represent the thermodynamically stratified nature of the atmosphere. Fig. 6 shows a staggered, block centered, numerical grid covering one octant of the Earth's surface (longitudes 0°–90° and Northern Hemisphere latitudes 0°–90°).

To determine unique solutions to the general circulation equations, GCMs require prescription of upper and lower boundary conditions. At the most basic level of GCM sophistication (see Manabe et al., 1965, for a seminal article in GCM simulation), such boundary conditions include: input of solar radiation at the top of the atmosphere, orography and land–sea distribution, albedo of bare land, surface roughness, and vegetation characteristics. Ocean conditions are modeled as either prescribed boundary conditions or calculated separately from either a simplified or an Ocean General Circulation model (OGCM). Currently, there are no synchronously coupled atmospheric-oceanic general circulation models (AGCM-OGCM) with sufficiently fine resolution (e.g. $100 \times 100$ km$^2$ grid cells) to simulate adequately regional hydrologic variables for the entire planet. In fact, even at coarser resolutions, fully coupled AGCM-OGCM simulations have not yet been successfully carried out. One basic limitation to this type of coupled climatic simulation is the range of relevant timescales. For the atmosphere these can be as short as a day or fractions of a day. For deep ocean circulation those timescales can be as large as 1000 years. One deeper, conceptual, impediment to fully coupled AGCM-OGCM simulations is the lack of a

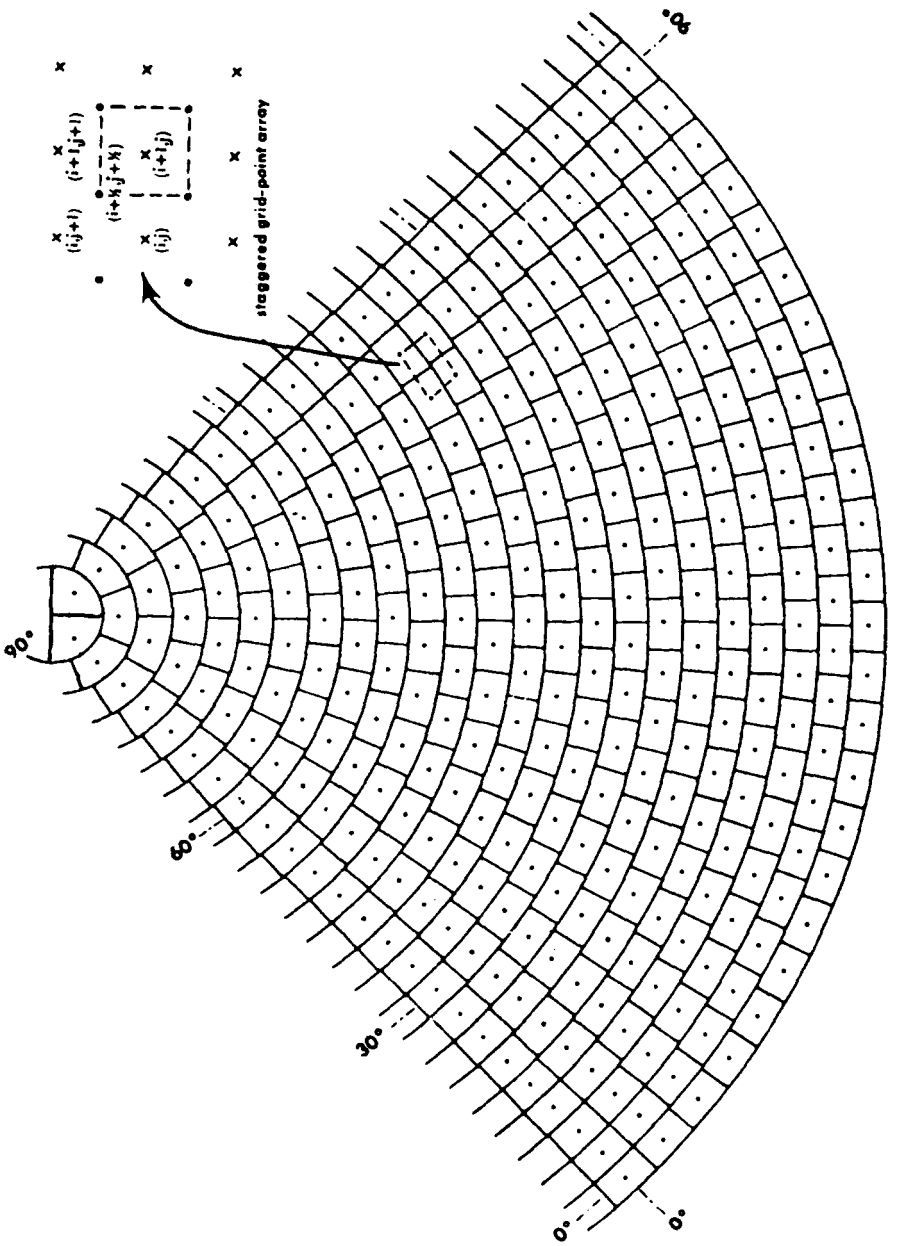


Fig. 6. A staggered GCM grid covering one octant of the Earth's surface (adapted from Peixoto and Oort, 1992).

basic understanding of how the land–atmosphere, ocean–atmosphere, and atmosphere–biosphere systems are coupled, hindering adequate parametrizations of key physical processes consistent with relatively fine GCM resolutions (say, $300 \times 300$ km$^2$ cell sizes). A variety of embedding or nesting schemes and subgrid parametrization schemes (Entekabi and Eagleson, 1989; Giorgi and Mearns, 1991) have been proposed to investigate the regional hydrologic impacts of induced greenhouse warming. This subject is pursued in a later section.

### 3.2. GCM predictions of global hydrologic impact

GCM simulations of the climate are either of the 'equilibrium' or 'transient' (time-dependent) type. Equilibrium simulations (the term 'shock' simulations is perhaps a better descriptor here) are conducted by abruptly doubling the atmospheric concentration of $CO_2$ relative to a base year. Subsequently, the climate evolution caused by that forcing is simulated until the surface–atmosphere system reaches a new radiative equilibrium.

Transient simulations (the term 'maintained perturbation' simulations may be a better descriptor in this case) impose a steady increase in $CO_2$ atmospheric concentrations, say, 1% year$^{-1}$ increase, while the climate of the Earth is synchronously simulated. Transient simulations typically incorporate the atmosphere–ocean coupling in some simplified fashion. The simulations are carried out to 100 years, routinely, and require that initial conditions be imposed on the climate to carry forward the GCM calculations. Transient simulations are relatively scarce compared with the equilibrium type, and make significant simplifications in their treatment of ocean dynamics (Washington and Meehl, 1989). A review of the literature on equilibrium and transient simulations of the climate revealed that the final predictions of global surface temperature increases do not differ fundamentally (see, e.g. Schlessinger and Jiang, 1991). Typically, the transient simulations yield a 100 year temperature warming that is a fraction of the equilibrium temperature reached by an abrupt doubling of $CO_2$. (The equilibrium temperature produced by an abrupt doubling of $CO_2$, denoted by $\Delta T_{2,x}$, which occurs $x$ years after that forcing is imposed, is called the climate sensitivity of the GCM.) That fraction varies generally between 60 and 95%, the larger percentage corresponding to GCMs with lower climate sensitivity. The equilibrium temperature $\Delta T_{2,x}$ occurs typically 5–15 years prior to the 100 year time horizon used in the transient simulations, and $\Delta T_{2,x}$ is reached faster in GCMs with high climate sensitivity.

GCM simulations of the climate forced by increased $CO_2$ seem to agree on one count (Mitchell, 1989; Ramanathan, 1988; Mitchell et al., 1990): the global mean surface temperature (base level of 1990 at 15°C) is likely to rise from 1.0 to 5.0°C by the mid 21st century. There is also general agreement in the CGM predictions of a likely cooling of the stratosphere. The amount of stratospheric cooling is less certain, but a range of 1°–6°C has been estimated, with the larger cooling occurring at the top of the stratosphere. The stratospheric cooling is caused mainly by ozone depletion by CFCs, and by increased infrared radiation (blackbody cooling) from the $CO_2$-rich stratosphere. Surface warming and stratospheric cooling are two greenhouse impacts

for which there is general consensus. The consensus is mostly on the sign of the greenhouse effect, rather than on the magnitude of the effect (see, e.g. Lindzen, 1990). As we have discussed, and will elaborate further later, the surface–atmosphere system is complex while the tools for climate prediction are too simplistic to put much confidence in numerical GCM results.

How do these general predictions of temperature changes caused by greenhouse warming relate to possible variations in the hydrologic cycle? Additional clues to this question might come from more involved, less certain, GCM predictions. These predictions (Intergovernmental Panel on Climate Change, 1990) suggest: (1) enhanced winter and spring warming in the high latitudes (above 50°) by a factor of 1.5–3.0 times the global surface average warming; (2) summer drying in continental northern midlatitudes; (3) surface temperature increases and their seasonal variations are least in the tropics. At a global scale, increased surface temperatures suggest higher evapotranspiration rates and, with the increment in associated precipitable water, increases of global average precipitation are estimated somewhere in the range of 3–15% from current levels (for a world-wide estimation of hydrologic cycle fluxes, see Zektser and Loaiciga, 1993). In other words, the induced greenhouse effect would intensify the global hydrologic cycle. Precipitation changes, however, are estimated to be minimal in the subtropical latitudes. In general, however, there is little agreement among GCMs about regional-scale precipitation changes. Because of the coarse resolution of GCMs, with grid cells generally over $300 \times 300$ km$^2$ in size, and the simplifications of the hydrologic cycle in those models, it is not possible to make reliable predictions of regional hydrologic changes directly from GCMs as a result of greenhouse warming. Nesting schemes where macroscale hydrologic models (MHM) are embedded into GCM grids have emerged as a possible way to discern regional hydrology from GCM results. Macroscale hydrologic models and nesting schemes will be treated in a later section.

### *3.3. Inherent hydrologic limitations of GCMs to model regional and global water cycles*

GCMs were conceptually designed to simulate average, large-scale, atmospheric circulation (see Holton, 1992). Variables predicted by GCMs are wind, temperature, humidity, surface pressure, precipitation, and the like, which are basic indicators of atmospheric conditions. There are other variables of key importance in hydrologic regimes, such as runoff and evapotranspiration which are not well represented by GCMs since they occur at model boundaries. Evapotranspiration, for example, represents an exchange of latent heat and water mass between the Earth's surface and the atmosphere. Its importance is demonstrated by the fact that at a global scale evapotranspiration is of the same order of magnitude as precipitation and runoff, the other two components of the long-term global water balance equation (Lvovitch, 1973). The process of heat and mass exchange between the surface and the atmosphere associated with evapotranspiration is not suitable for modelling as a boundary condition, because transfer at the Earth's surface affects the atmosphere, which, in turn, affects transfer processes at the surface. Consequently, estimation of runoff from GCM output as the difference between precipitation and evapo-

transpiration (see, e.g. Oki et al., 1993) is bound to be inaccurate at all scales of spatial resolution when evapotranspiration is not properly modelled. In the terrestrial environment, physically based, parametrized, soil–vegetation–atmosphere transfer schemes (SVATS, Shuttleworth, 1993) have emerged in an attempt to model better the land–atmosphere interactions at regional scales. Examples of macroscale hydrologic modeling of land–atmosphere interactions, and of the nesting of these models within GCMs, are the biosphere–atmosphere-transfer scheme (BATS, Dickinson et al., 1986; Dickinson, 1989) and the simple biosphere (SiB, Sellers et al., 1986, 1989) model. Macroscale hydrologic models and their interfacing with GCMs will be elaborated upon further in a subsequent section.

## 4. Feedbacks on greenhouse warming

Fig. 7 shows a simplified version of a series of climate feedbacks that are believed or

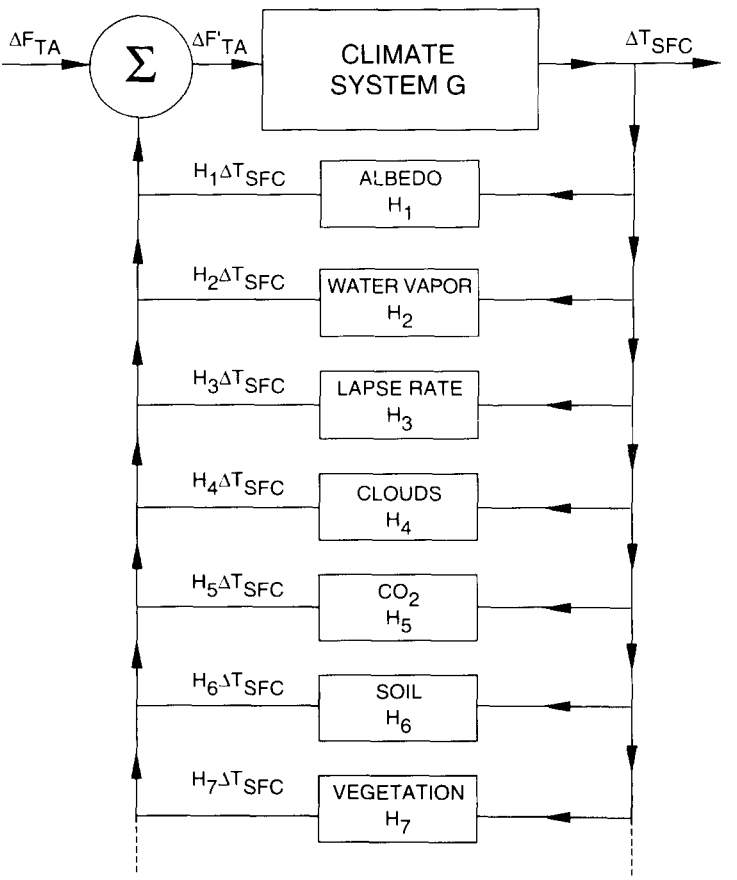


Fig. 7. Climate system feedbacks (adapted from Peixoto and Oort, 1992).

known to arise as a result of forcing of the global climate by greenhouse warming. Using a representation common in systems control engineering, the greenhouse forcing by gases such as $CO_2$ on atmospheric temperature ($\Delta F_{TA}$) affects the climate system to change surface temperature ($T_{SFC}$). This increase in temperature, however, triggers a series of 'feedbacks' in the climate system that accentuate (positive feedback) or diminish (negative feedback) the greenhouse forcing. These climate feedbacks are moreover highly non-linear, with some feedbacks affecting other feedbacks (interfeedback interaction is not represented in Fig. 7).

### 4.1. Water vapor feedback

The possibility of a water vapor feedback on climate, represented in Fig. 8, seems to have been raised as early as 1897 by Chamberlin (Chamberlin, 1897). This is one of the most closely investigated feedbacks owing to its likely prominent role in climate change. It is one of the few feedbacks for which there is general consensus on the sign of its effect (in fact, positive) on climate forcing. Starting the analysis of this feedback cycle at step 1 (arbitrarily), increased atmospheric $CO_2$ concentrations result in increased infrared emissions to the Earth's surface, raising its temperature ($T_M$, in Fig. 8) directly. The heat gain in the mixed layer evaporates more water from the oceans and land, and atmospheric (absolute) humidity rises. Simultaneously, latent heat is transferred to the atmosphere by the evaporated water, raising the tropospheric temperature ($T$) after water vapor condenses. Tropospheric temperature is also raised by the absorption of infrared radiation by $CO_2$ (and other greenhouse gases, process 2 in Fig. 8). The greater tropospheric temperature, in turn, enhances the water-holding capacity of the atmosphere and hence its humidity. Water vapor, an effective greenhouse gas, traps infrared radiation, and along with the warmer troposphere as a whole, increases infrared emissions back to the mixed layer, heating it up further. This heat input contributes to surface evaporation, completing the feedback loop of water vapor (diagram 3 in Fig. 8).

Blackbody cooling by the warmer surface–atmosphere system impedes runaway

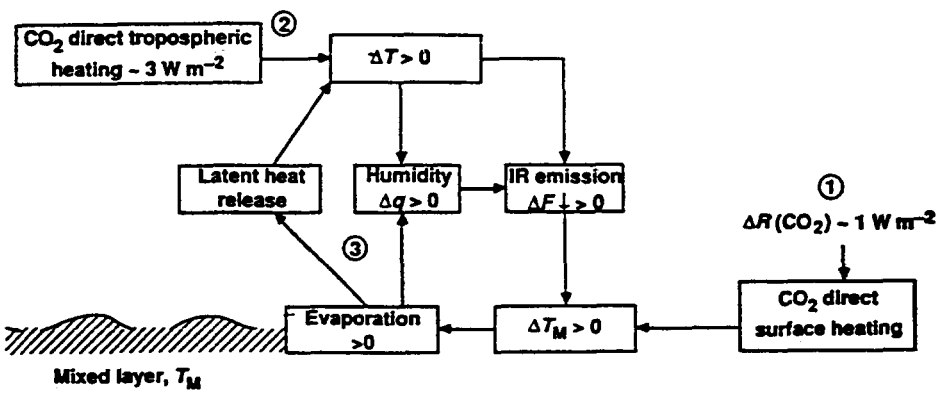


Fig. 8. An abstract representation of the water vapor feedback (after Ramanathan, 1988).

warming of the Earth's surface, as explained earlier. In addition, the water vapor feedback forcing has its own natural 'brakes'. Modifications in the lapse rate (which originates the lapse-rate feedback shown in Fig. 7) have been identified as being one of these 'brakes'. As the vertical profile of water vapor is shifted upwards by increased humidity in the warmer troposphere, there is an ensuing convection of heat away from the surface towards higher altitudes. As a result, the lapse rate (the rate of atmospheric temperature change with altitude) decreases (see, e.g. Ahrens, 1994). This process is likely to be accentuated in the tropics, as the lapse rate there is close to moist adiabatic, and the moist adiabatic lapse rate decreases with higher temperature. Since the surface is typically warmer than higher altitude air, it follows that, at least in tropical areas, the surface air may warm less than upper tropospheric air. This is caused by (1) the preferential transfer of heat toward higher altitudes resulting from the shift in water vapor profile, and (2) by lapse rate differentials at low and high elevations. It seems then that the lapse-rate feedback is negative, thus acting to lower surface temperature and tempering the (positive) water vapor feedback.

### *4.2. Cloud feedback on the climate*

Great uncertainty surrounds the impact of induced greenhouse warming on the Earth's cloud systems, and how, in turn, the potentially changed clouds will effect the climate (this is the cloud feedback of greenhouse warming, Weatherald and Manabe, 1988; Ramanathan et al., 1989a; Raschke, 1993). It is known, however, that in the present climate, with a global mean cloudiness of close to 50%, clouds have both a positive forcing, i.e. they trap infrared radiation and contribute to surface warming, as well as a negative forcing. Negative forcing occurs by the reflection of incoming solar radiation back to space, thereby reducing the flux of energy reaching the surface relative to clear-sky areas. Results from the ERBE (Ramanathan et al., 1989a,b; Harrison et al., 1990; Ramanathan and Collins, 1991) indicate that in the present climate, the clouds have an overall net negative forcing effect, that is, they reflect more shortwave radiation than they trap infrared radiation. The global mean net cloud forcing has been estimated at about $-16$ W m$^{-2}$ (Ramanathan et al., 1989a). Conversion of this radiative forcing to surface heating depends on the climate model used for this purpose, but it is estimated that the net cloud forcing is responsible for a surface temperature that is between 10° and 15°C cooler that it would otherwise be. For comparison purposes, it is estimated that if atmospheric concentrations of $CO_2$ were increased from 300 ppmv to 600 ppmv, the infrared radiative trapping would be close to 4 W m$^{-2}$, with a concomitant surface warming on the order of 2°–4°C.

Interestingly, in spite of the increased atmospheric humidity bound to occur in a warmer climate, most GCMs predict a decrease in global mean cloud cover under that condition (Cess et al., 1990). The relevant physics behind this surprising prediction appear to be increased drying in the upper troposphere by cumulus subsidence (Lindzen, 1990) and midlatitude moisture flux divergence (Del Genio, 1993), both of which act to inhibit cloud formation and offset increased atmospheric moisture under greenhouse warming. Consequently, because of the strong albedo effect of

clouds (they reflect solar radiation), the overall predicted drop in cloudiness has a net positive (warming) feedback on the climate, according to most GCMs. In other words, the cloud cover feedback of greenhouse warming appears to be positive according to various GCM simulations.

GCMs are too simplistic in their treatment, via parametrization schemes, of cloud physics. Issues that are not properly modeled by GCMs in relation to cloud feedback include the possible diurnal (e.g. day to night) and seasonal (summer to winter) cloud shifts, changes in latitudinal cloud cover (low latitudes to high latitudes), cloud cover shifts involving surface albedo variations (from dark, oceans or forests, to bright, desert or snow, surfaces), and changes in cloud optical thickness (Del Genio, 1993).

It is clear from our discussion of the water vapor and cloud feedbacks, that there is a strong interaction between them, as well as with the lapse rate and surface albedo feedback. The variations in atmospheric humidity, which are the result of changes of the radiation balance under greenhouse warming, play a central role in the ultimate equilibrium state of a potential warmer climate.

### *4.3. Surface albedo, soil moisture, and vegetation feedbacks*

Surface albedo, soil moisture, and vegetation feedbacks share some common characteristics. All are processes at the surface–atmosphere interface. Soils and vegetation integrate the biosphere as an important part of induced greenhouse warming. The roles of soils and vegetation in the climate-change puzzle are poorly understood at this point. Most of what is currently predicted about their likely role as feedback forcing mechanisms in induced greenhouse warming is derived from GCM simulations. The GCM parametrizations of soil and vegetation processes, however, are particularly difficult to calibrate and validate.

Fig. 9 illustrates the likely processes involved in a soil-moisture feedback. This feedback is bound to occur in regions where precipitation is predicted to decline, at least seasonally, such as during the summer in central North America. Thus, the soil-moisture feedback is of regional scope, in contrast to, say, surface warming or increased humidity, which are global in nature. With lower precipitation and a warmer surface (point 1 in Fig. 9), the soil surface becomes drier (point 2 in Fig.

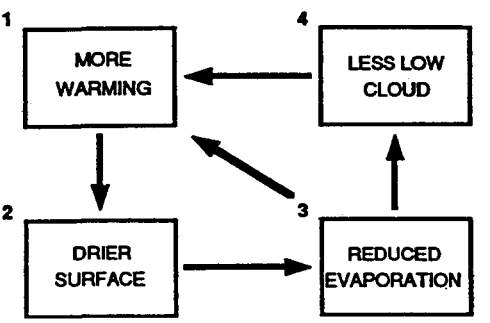


Fig. 9. An abstract representation of the soil-moisture feedback (after Mitchell et al., 1990).

9). Evapotranspiration is reduced as the soil moisture drops resulting in lower cloud formation. As evapotranspiration declines, so does the evaporative cooling associated with the latent heat removal from the surface. Lower cloud formation enhances surface warming as the atmosphere becomes less reflective to solar radiation. The reduced evaporative cooling (step 3 in Fig. 9) and the enhanced transparency of the atmosphere to shortwave radiation (step 4 in Fig. 9) start the soil-moisture feedback on surface warming, which is positive according to this reasoning.

The surface albedo feedback refers mainly to ice-mass modifications in a warmer climate. A warmer climate, with surface temperatures magnified at high latitudes according to GCMs, melts ice and snow. These two surfaces are more reflective than water or land surfaces generally. Therefore, a warmer climate may reduce the planetary surface albedo (ratio of reflected over incoming shortwave radiation), thus increasing absorption of incoming solar radiation, which, in turn, warms the surface further, giving rise to the ice-albedo feedback. The effect would be most severe at sea–ice margins and polar regions, stressing the regional character of the albedo feedback.

Vegetation feedbacks on climate involve the biosphere in a major way, and are poorly understood (Manabe and Wetherald, 1987). The vegetation feedback resulting from surface warming may be triggered by changes in vegetated areas and types of vegetative cover. These changes, in turn, could affect the surface–atmosphere temperature directly (say, by modifying the surface albedo), or through modifications in the $CO_2$ exchange between the atmosphere and the surface. Plant growth and respiration depend critically on atmospheric $CO_2$, ambient temperature, and soil moisture. The interplay of these variables introduces many degrees of freedom and uncertainties in the biosphere–climate system. Consequently, prediction of even the sign of vegetation feedbacks on greenhouse warming at regional scales is currently infeasible. Deforestation, not a climate feedback per se, but rather, a deliberate stress on the biosphere–climate system, has the potential to reduce regional precipitation rates by as much as 20%, as shown by recent studies (see, e.g. Dickinson, 1989).

The previous discussion of various potential feedback mechanisms of greenhouse warming reveals that, except for the case of ice albedo, evaporation is a critical mechanism by which feedbacks are induced following surface warming. The complexity of the interactions between the atmosphere, land, and oceans makes it virtually impossible to develop an accurate picture of how the Earth's climate might ultimately evolve in a warmer Earth. From a hydrologic perspective, however, the consequences of greenhouse warming go beyond mere surface warming. Seasonal modifications in precipitation and runoff are two areas of special significance for water supply. Amplification of the magnitude of floods and severity of droughts are areas of special concern, also.

### *4.4. Ocean–atmosphere interactions*

The interaction of oceans and the atmosphere is perhaps the single most important factor, after the Earth's rotational motion, governing general atmospheric circulation. Yet, as has been stated earlier, the ocean–atmosphere coupling is the least

understood and least prone to accurate numerical modelling. Fig. 10 shows a simplified representation of some of the interactions in the ocean–atmosphere system, some of which are likely to trigger significant climate feedbacks in a warmer planet.

Thermohaline circulation of the oceans is driven by density gradients in ocean water that result from variations in seawater temperature and salinity. Fig. 10 presents a hypothetical situation where the freshwater flux ($H$), at the top of Fig. 10, to oceans in the high latitudes (specifically in the North Atlantic, see, e.g. Toggweiler, 1994) is perturbed, say, by increased precipitation in a warmer climate. The potential mixing of freshwater and ocean water results in reduced salinity and, thus, lower seawater density. Consequently, the sinking motion of ocean water decreases, and, with it, the meridional circulation of ocean water. The polar salinity is further reduced by the potential decrease of saltier water flux from lower latitudes (loop 1 in Fig. 10). As the poleward transport of relatively warm water is reduced, it induces a drop in the surface temperature at high latitudes. This completes a negative-feedback on greenhouse warming in the polar regions (loop 3 in Fig. 10). Note, again, how the hydrologic cycle could (through salinity reductions induced by greater precipitation) impact the equilibrium surface temperature. It is likely that the temperature drop exerted by the aforementioned negative feedback will steepen the poleward atmospheric convective heat transport ($\tau$ represents momentum flux in Fig. 10) and the air–sea heat flux ($Q$) exchange, partly offsetting the salinity-induced negative feedback.

As surface temperature in the high latitudes and polar regions declines, evaporation will do so, also. This reduces salinity (loop 2 in Fig. 10), which, in turn, could further reduce meridional ocean circulation and affect poleward heat transport through ocean–atmosphere coupling. The ultimate effect of the feedback in loop 2 depends

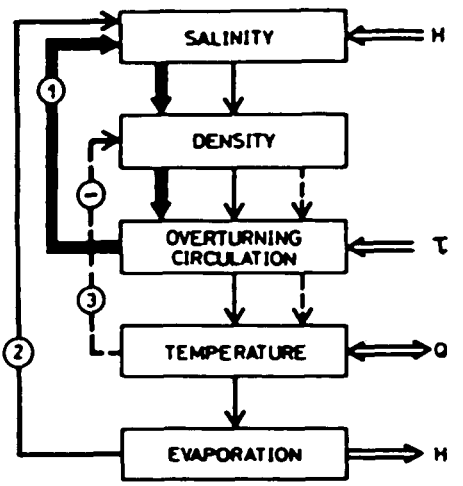


Fig. 10. Abstract representation of coupled ocean–atmosphere–hydrologic cycle processes in the high latitudes (after Willebrand, 1993).

on the fate of precipitation over the regions under consideration at the relevant timescales of oceanic circulation. For example, if precipitation decreases over these high latitudes, then the feedback in loop 2 is largely neutralized, since lower ocean–freshwater mixing tends to reinstate the salinity levels lowered by reduced evaporation.

The discussion of the hypothetical scenarios in Fig. 10 illustrates the complexity of interactions between greenhouse warming, changes in the hydrologic cycle (precipitation and evapotranspiration), oceanic circulation, and atmosphere–ocean coupling.

## 5. Macroscale hydrologic modelling

Current prediction of climate evolution under greenhouse warming relies on GCM simulations. The most detailed global-scale simulations typically use grid cells larger than 2.5° × 2.5°. Given the Earth's radius (6371 km), this means a resolution of close to 300 km for hydrologic variables such as precipitation. This scale of spatial averaging is inadequate for representing short-term (on the scale of days) hydrologic processes, especially over continental land masses. A variety of nesting schemes have been devised in an attempt to extract hydrologic information useful at the river-basin scale from GCM results. These schemes are referred to by names such as Limited Area Meteorological models (LAM, Giorgi and Mearns, 1991), Macroscale Hydrologic models (MHM, Vorosmarty et al., 1993), or subgrid parametrizations (Entekabi and Eagleson, 1989; Wood et al., 1992), each with its own idiosyncrasies. The nesting of macroscale hydrologic models within GCMs introduces several issues of key importance: spatial scaling, timescaling, parametrizations of hydrologic processes, and model calibration/validation. Let us examine these in more detail.

### 5.1. Spatial and time scales

Table 2 provides examples of the various time and spatial scales that are

Table 2
Characteristic spatial and temporal time-scales for hydrologic and atmospheric processes.

| Hydrologic scales | | | |
|---|---|---|---|
| Scales | Santa Ynez river | Colorado river | Amazon river |
| Space | 10 km | 100–1000 km | 100–10 000 km |
| Time | 1–10 days | 10–100 days | 100–1000 days |
| Atmospheric phenomena | | | |
| Scales | Thunderstorms | Hurricanes | Synoptic droughts |
| Space | 1–10 km | 10–100 km | 100–1000 km |
| Time | 1 h–1 day | 1–10 days | 100–1000 days |

encountered across a broad spectrum of river basins and atmospheric phenomena. River basins vary from the small (spatial) scale (for example, Santa Ynez river of Santa Barbara County, California, tributary area of approximately 1000 $km^2$), to the medium-size, regional-scale (Colorado river of the United States, tributary area of approximately 640 000 $km^2$), to the continental scale (Amazon river, with the largest tributary area, 6 150 000 $km^2$, and largest mean annual runoff in the world). The timescales shown for each of these hydrologic basins represent typical time periods over which direct runoff and baseflow hydrographs tend to stabilize following regular variations from mean flow conditions.

The time and spatial scales for atmospheric phenomena in Table 2 are representative of weather and climatic forcings to hydrologic regimes. General circulation models are better suited to predict the large-scale synoptic phenomena. Transient phenomena that occur at smaller spatial scales, such as hurricanes and thunderstorms, are ordinarily better modelled by limited-area meteorological models. The prediction of runoff by GCMs is rather crude, as will be seen later, leading to significant errors in runoff prediction at the continental and regional scale. GCMs can not 'see' the smaller scale river basin because of their coarse grid resolution. Subgrid hydrologic models are needed to resolve the larger scale GCM predictions and predict smaller scale hydrologic phenomena (Hostetler and Giorgi, 1993).

### 5.2. *Adaptive multigrid coupling of GCMs, meteorologic, and hydrologic models*

Fig. 11 illustrates the concept of adaptive multigrid methods for nesting

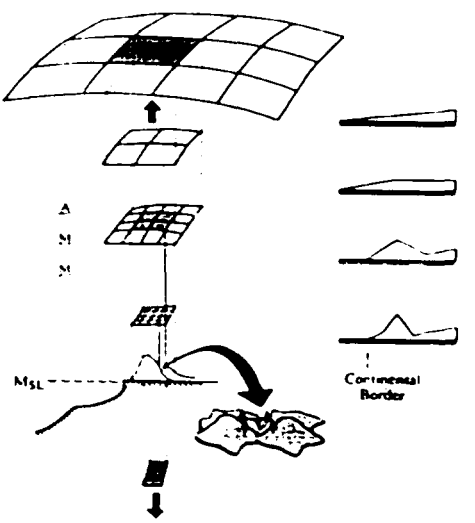


Fig. 11. Multigrid nesting for general circulation models (GCMs), Land Atmosphere Meteorological (LAM) models, macroscale hydrologic models (MHMs), and landscape-scale hydrologic models (LSHMs) (after Barros and Lettenmaier, 1993).

hydrometeorological methods of increasingly finer resolution on the host grid of a GCM. The increasing resolution achieved by the smaller scale models permits a more accurate representation of physiographic characteristics and the parametrizations of important surface-controlled processes such as evapotranspiration. Grid nesting is implemented by solving, numerically, the standard equations of continuity, momentum, and heat conservation, plus related state equations for key variables such as moisture, precipitation, wind speed and direction, pressure, temperature, etc., in the GCM. The GCM approximations within a particular simulation's time step serve as a boundary condition or an initial condition, or both, to the higher resolution model nested within it. The nested or subgrid model is then simulated based on the GCM approximations to produce its own set of results. For example, the GCM simulation for atmospheric moisture, upper tropospheric temperature, and wind speed in a given time interval, might be used by a limited area meteorological (LAM) model to estimate precipitation distribution over a zone covered by the GCM's grid.

Table 3 shows some of the possible variants of the nesting or multiple-scale approach. Starting at the continental scale in Table 3, a GCM is interactively linked with a macroscale hydrologic model (in this case the latter with a spatial scale of 10–50 km). The GCM grid produces averaged estimates over cells larger than 100 km in side size. At the continental scale, the GCM might utilize subhourly time steps. The estimated variables at this level of time resolution are then input to the macroscale hydrologic model which produces integrated (i.e. by time-averaging) variables with a time-resolution of weeks or months in this case. The link between the GCM and the macroscale hydrologic model is interactive in the sense that as the simulation in the GCM progresses, inputs to the macroscale hydrologic models are updated. Vorosmarty et al. (1993) indicate that the interaction between the GCMs and the macroscale hydrologic models does not have to be necessarily of the 'top-down' type. They suggest the possibility of propagating physically valid dynamics from local and regional scales to the synoptic-scale levels of the GCMs, thus creating a coupled 'top-down' and 'bottom-up' linkage between the various models.

Table 3
Scales and resolutions of models for hydrologic simulation of climate change forcings (adapted from Vorosmarty et al., 1993)

| Scale | Model | Boundary | Resolution | |
|---|---|---|---|---|
| | | | Atmosphere | Hydrology |
| Continental | Linked GCM–MHM | Interactive in GCM | $\geqslant$100 km (subhourly) | 10–50 km (weekly to monthly) |
| Meso (Regional) | Linked meso–MHM | Prescribed or interactive in nested GCM | 10–50 km (minutes) | 1–10 km (daily) |
| Local | Hillslope–small catchment | Topographically determined | Prescribed point forcings (subdaily) | $\leqslant$1 km (subdaily) |

At the second level of scales in Table 3, a mesoscale atmospheric model (10–50 km spatial resolution, which is nested with the synoptic-scale GCM) is interfaced with a macroscale hydrologic model with a spatial resolution of 1–10 km. The hydrologic model output is integrated over a daily time step, whereas the mesoscale inputs to it are resolved over a timescale on the order of minutes. Note that the GCM inputs to the atmospheric mesoscale model can be either interactively updated or prescribed, i.e. fixed during the simulation period of interest. The third level of scale in Table 3 is local. Here, a catchment is simulated at the 1 km or smaller spatial scale, with physiographic characteristics representable by a digital elevation model. The catchment response is driven by precipitation forcings prescribed with subdaily station data. Fig. 12 graphically depicts the interaction and nesting of the variable scales models conceptualized in Table 3.

### 5.3. *Land–atmosphere parametrization of hydrologic processes*

From our previous discussion of GCMs, it is clear that, in addition to dynamic coupling of the ocean–atmosphere system, coarse grid resolution and land–atmosphere coupling pose the greatest obstacles to the accurate prediction of hydrologic variables (principally runoff and evapotranspiration) at regional and local scales. A great deal of effort has been devoted over the last few years to develop adequate parametrizations of soil–vegetation–atmosphere interfaces. The hydrologic processes of greatest relevance here are the exchange of water vapor, heat, and momentum at the land–atmosphere interface, which involves soils, vegetation, and the lower atmosphere. These surface hydrologic processes are determined by soil and vegetation characteristics, subsurface geology, and landscape features, as they control surface albedo, soil moisture, surface roughness, and stomatal roughness

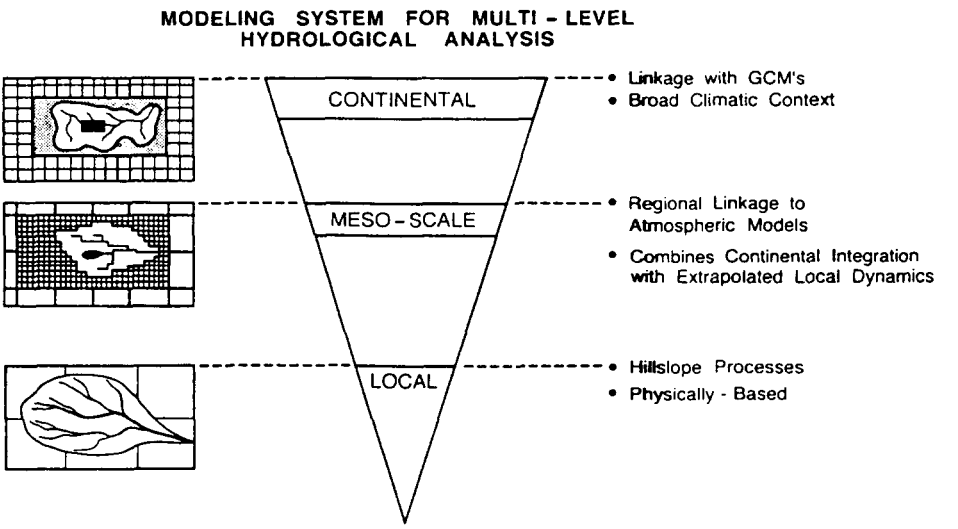


Fig. 12. Modelling system for multilevel hydrological analysis (after Vorosmarty et al., 1993).

(Avissar and Verstraeter, 1990; Shuttleworth, 1993). A parametrization of surface hydrological processes consists of a simplified representation of the various intervening reservoirs of water and sources of heat, the fluxes of water exchange and rates of heat transfer among them, and a set of state and/or empirical equations that approximate water-phase transformations and rates of mass and heat transfer. Parameters are introduced that may represent macroscopic averages of molecular and small-scale interactions. These parameters are simplificatory in nature and in many cases they are accessible to measurement, or to calibration by measurement. Examples of such parameters are surface roughness, stomatal roughness, turbulent and diffusion coefficients, to cite a few with physical connotations.

Manabe (1969) reported what appears to be the first numerical parametrization of the hydrologic cycle within a GCM. Fig. 13 shows Manabe's (1969) simple bucket model of land surface hydrology. The simple bucket model of Fig. 13 assumed that if precipitation exceeded evaporation then the soil 'bucket' would fill up. If the soil reaches saturation, then runoff occurs. (In truth, hydrologic theory establishes that runoff occurs if the rate of precipitation exceeds the rate of infiltration, for any degree of soil saturation.) As long as the soil was at or near saturation the actual evaporation rate would be equal to the potential evaporation rate (Manabe's bucket model did not consider vegetation). Otherwise, the actual evaporation ($E$) would be proportional to the potential rate ($E_p$), $E = \beta E_p$, the parameter $\beta$ being the rate of proportionality. $\beta$ was simply equal to the ratio of current soil moisture to field capacity ($\beta \leqslant 1$).

This first generation of hydrologic (simple bucket) parametrizations has been superseded by more complex and realistic models of surface hydrologic processes used in conjunction with atmospheric circulation models. They are generally

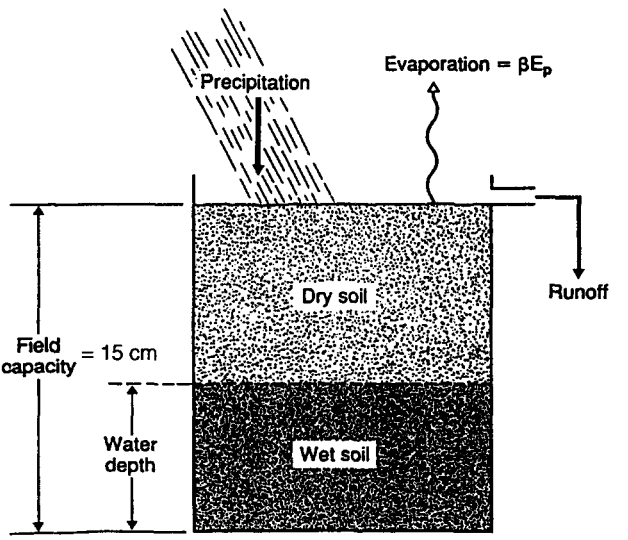


Fig. 13. Representation of Manabe's simple bucket hydrologic model for a GCM (adapted from Shuttleworth, 1993).

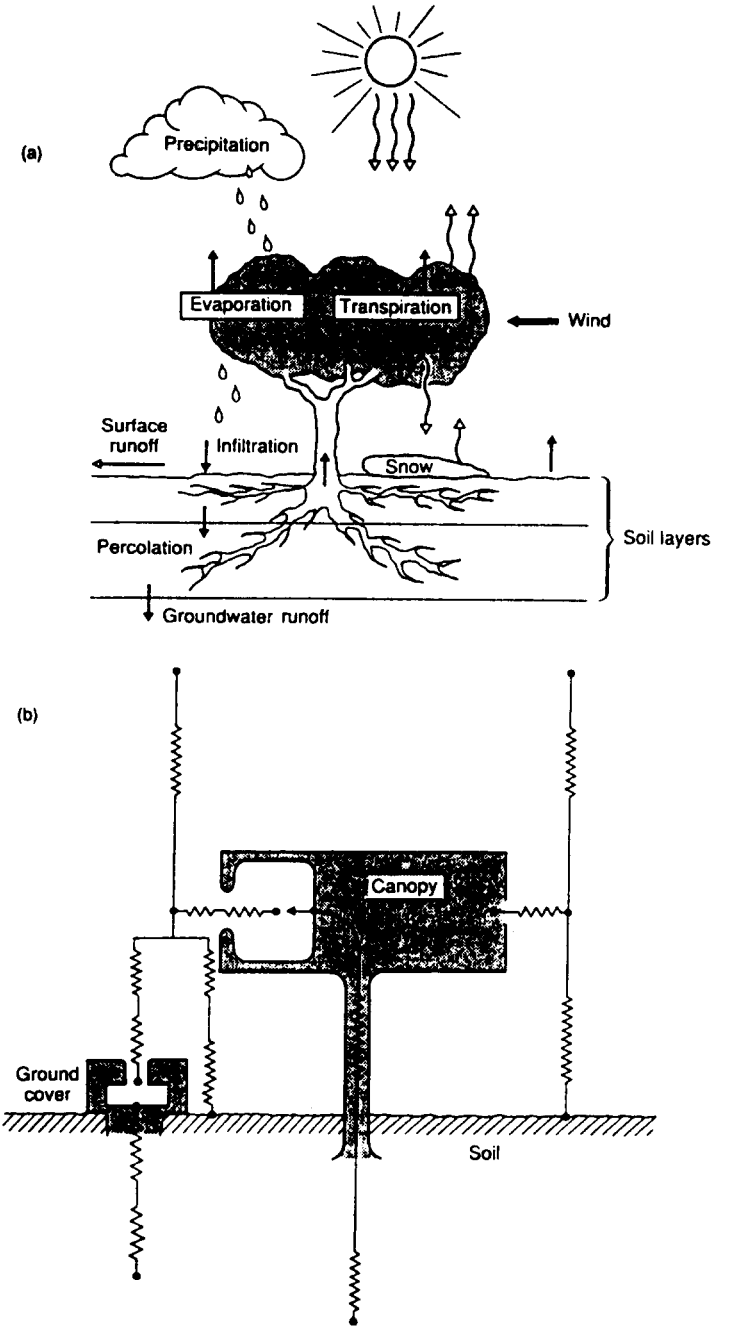


Fig. 14. (a) Representation of Dickinson et al.'s (1986) BATS model; (b) representation of the SiB model by Sellers et al. (1986) (after Shuttleworth, 1993).

known as Soil–Vegetation–Atmosphere–Transfer schemes (SVATS). Fig. 14, shows two variants of SVATS, the Biosphere–Atmosphere Transfer Scheme (BATS, Dickinson et al., 1986, in Fig. 14(a)), and the Simple Biosphere (SiB, Sellers et al., 1986, Fig. 14(b)). These models include layered parametrizations of the vegetation structure (ground cover and overstorey) and of the soil. The SVATS conduct radiative transfer calculations considering vegetation and soil conditions for given inputs of incoming solar radiation. Soil heat transfer, sensible heat transfer, evapotranspiration, and precipitation interception in the overstorey are modeled by the SVATS. Evapotranspiration estimation considers the effect of light, temperature, vapor pressure deficit, leaf water potential, and soil moisture around the root zone on canopy's stomatal resistance. The representation of the SiB model in Fig. 14(b), shows how the vertical transfer of mass, momentum, and heat is conceptualized as a series of flow paths each with its own 'resistance' (analogous to Ohm's law describing the resistance to electrical currents in a conductor, as advocated by Monteith, 1973), in soil and canopy layers. Interaction is allowed between the canopy and ground cover, as the overstorey imposes additional resistance to transfer from the ground cover and the soil top layer to the atmosphere. These resistance parameters are obtained from basic canopy, leaf, and soil structure.

For given precipitation and meteorological GCM inputs (humidity, wind speed, surface temperature, solar radiation), the SVATS can calculate evapotranspiration and deep percolation, and, thus runoff, within a grid cell of the SVATS numerical model. Addition of runoff so calculated over the SVATS model grid cells spanning a river basin can yield the calculated total river runoff over sufficiently long periods, such as 1 year. This is, in fact, the procedure followed to calculate annual runoff in GCMs. Runoff calculations over shorter time steps, such as 1 month, may not be additive over all grid cells in large river basins. This is due to the delay caused by the traveltime of streamflow through the channel network, which precludes contemporaneous cell-runoff summation to estimate basin-wide runoff. GCMs that are not interfaced with SVATS or some other surface hydrologic model resource to cruder schemes to runoff calculation. Routinely, precipitation over individual GCM grid cells is converted to runoff by empirical rules (Miller and Russell, 1992). Runoff prediction is examined in more detail in a later section.

It would be naive to assume that the degree of added complexity in SVATS has resolved the basic problem of surface hydrology modeling in GCMs. SVATS must be parametrized in such a way that they are applicable globally (i.e. for any terrestrial biome around the planet), and, yet, are able to accommodate different ground covers. This necessitates the introduction of parameter sets tuned up for specific land covers (e.g. tropical humid forest, boreal forests, steppe grasslands, etc.). It is not possible at present to mix different vegetation covers within a single SVATS grid cell, as SVATS models assume physiologically uniform vegetative cover over level terrain. Lastly, there remains the nagging issue of coarse grid resolution in the GCMs which determines important inputs to the SVATS, such as average precipitation and wind speed over the GCM cells. In spite of these hurdles, the interfacing of SVATS with GCMs has added new capabilities for regional hydrologic modelling, as exemplified by the tropical deforestation studies by Dickinson and Henderson-Sellers (1988), among

others. The area of land–atmosphere hydrologic modeling constitutes one of the most vibrant fields of hydrology today.

### 5.4. GCMs, macroscale hydrologic models, SVATS, and validation

One of the tenets of the scientific method is hypothesis testing through experimentation and observation. In the case of induced greenhouse warming, hypothesis testing is not a straightforward matter, simply because most of the predicted effects, hydrologic or otherwise, are transient and are not expected to become fully manifested until after a few decades. For example, global yearly precipitation is predicted by various GCMs to increase on the order of 10% of the current mean as the Earth's surface warms up. Yet, a mean surface temperature increase of about 2°C is not expected to be realized until the middle of the 21st century (Intergovernmental Panel on Climate Change, 1990), or further away than that.

Consider next the much more complicated subject of regional hydrologic changes, of which seasonal modifications in precipitation and runoff are of central interest. Runoff and precipitation at regional scales are highly variable, with 10–20 year averages commonly fluctuating in the range ±25% of their long-term means (Amorocho and Espildora, 1973; Klemes, 1991; V. Klemes, personal communication, 1994). Yet, yearly changes in precipitation in a warmer climate are predicted to be on the order of +10% of the current average. It is clear that there is a signal-to-noise ratio detection problem here. The change in the signal that is to be detected (say, +10% in precipitation) is significantly smaller than the natural variability of the signal known to exist (see Loaiciga et al. (1993), for an analysis of long-term hydrologic variability). At smaller timescales the signal-to-noise detection problem is likely to worsen, as inherent hydrologic variability increases over shorter time averages. This point has been demonstrated by Briffa et al. (1990) in a study of summer temperatures in Fennoscandia via a 1400 year long tree-ring reconstruction of temperatures in that region. Briffa et al. (1990) showed that it would take between 30–40 years (counted after 1990) to identify a global warming signal in the form of increased summer temperature. To compound matters, analyses of existing precipitation and runoff records report somewhat conflicting results. For example, Karl et al. (1991), based on an analysis of 20th century precipitation in the central United States, found no statistically significant trends in winter precipitation. (This is at odds with GCM predictions that posit winter precipitation increases with an enhanced greenhouse effect, Intergovernmental Panel on Climate Change, 1990). Yet, Lins and Michaels (1994), using streamflow data from 1941–1988 from 559 gages across the United States, determined that winter and autumn unimpaired streamflow showed statistically significant increasing trends across the gamut of hydroclimatic regions used to subdivide the coterminous United States. Lins and Michaels (1994) speculate that the reason for increasing winter runoff while there is no contemporaneous increase in precipitation in the central United States must be a decrease in evapotranspiration over this area.

Hydrologic theory provides methods for calibrating and validating hydrologic models under constant or changing conditions (Klemes, 1985), the latter occurring

in a transition to a warmer climate in this instance. Under changing conditions, however, the task of model calibration and validation is difficult. To be specific, consider Table 4, summarizing a general hierarchical scheme proposed by Klemes (1986). On a scale of increasing difficulty, calibration and validation of a hydrologic model is simplest under constant climatic conditions when a model is calibrated in a basin and validated in that same basin. This gives rise to the split-sample test in Table 4. The available hydrologic record for basin A should be split into two non-overlapping records. One record is used for model calibration and the other for model validation. If possible, the two records should be reversed, so that two-split sample tests can be performed. The model is considered acceptable only if the model validation results, in both cases, are acceptable (see Amorocho and Espildora (1971) for model calibration and validation criteria). If the hydrologic record is too short to be split, or for some other reason cannot be split, then other tests may be entertained. The proxy-basin test for geographic transferability is one such alternative test. This test is required for any model which is assumed to be geographically transferable within a region hydrologically and climatically homogeneous. If the goal is to simulate streamflow for an ungaged basin C, then the model to be used should be tested on two gaged basins A and B. The model should be calibrated on basin A and validated on basin B and vice versa. Only if both proxy-basin tests are acceptable should one consider the model as geographically transferable.

Moving up the scale of difficulty in Table 4, we find the differential split-sample test for climatic transferability. This test applies for testing hydrologic models under conditions different to those used to calibrate them. The basic idea behind this test is to split the record into different climatic regimes and to demonstrate the ability of the record to perform adequately under the particular climatic transition under consideration. For example, if the objective is to simulate streamflow under very wet climatic conditions, then the model should be calibrated on a dry portion of the hydrologic record and validated on a wet portion of the historical record. Such differential split-sample tests evaluate the ability of a model to perform adequately under the climate conditions considered.

The most involved model test is the proxy-basin differential split-sample test for geographic, land-use and climatic transferability. Such broad transferability is probably the ultimate objective of most hydrologic models. The test aims, for

Table 4
Hierarchical approach for operational testing of hydrologic simulations

| | Constant conditions | | Transient conditions | |
|---|---|---|---|---|
| | Basin A | Basin B | Basin A | Basin B |
| Basin A | Split-sample test | Proxy-basin test | Differential-split-sample test | Proxy-basin differential split-sample test |
| Basin B | Proxy-basin test | Split-sample test | Proxy-basin differential-split-sample test | Differential-split-sample test |

example, at assessing whether a model calibrated to a dry climate on basin A can simulate streamflow for a wet climate on basin B, and vice versa. The differential split-sample test and the proxy-basin differential split-sample test are clearly called for in testing hydrologic models embedded in GCMs, such as the SVATS previously discussed. Changes in climate justify using these complex model-testing methodologies. The obvious shortcoming here is the lack of available data bases to conduct these tests over a representative cross-section of regions and varying climatic conditions. Paleoclimatic reconstructions of precipitation, temperature, runoff, and vegetation (Loaiciga et al., 1993; Swart et al., 1993), in spite of all their inherent approximations, offer in many cases the only source of information upon which to test hydrologic models over changing conditions.

Another significant obstacle to hydrologic model testing under a climate change is the likely presence of climatic feedbacks (see Fig. 7). These feedbacks may modify the essence of the hydrologic regime, thereby rendering parametrization under the current climate unrepresentative of the hydrologic response under different climates. A case in point is vegetation change caused by climate change, which might in turn modify the regional climate. In this case, the vegetation feedback must be properly accounted for in the GCM. This situation is reminiscent of the 'top-down'/'bottom-up' interfacing of GCMs and macroscale hydrologic models discussed earlier. In short, testing of hydrologic models embedded in GCMs may require testing of the GCM also.

## 6. Examples of hydrologic simulation under climatic change

The approach to assessing changes in regional climate and hydrologic regimes caused by greenhouse warming has been outlined above. Hydrologic models are embedded within GCMs or synoptic-scale atmospheric models. This nesting scheme permits, at least in concept, narrowing down the scale of hydrologic simulation to the catchment level. The literature on this subject matter is by now rather extensive (Rind et al., 1992). Early work was reported by Gleick (1986, 1987). Dickinson and Henderson-Sellers (1988) studied the effects of deforestation via GCM simulation. Lettenmaier and Gan (1990) simulated seasonal runoff and its variation in selected California river basins under the equilibrium climate ($2 \times CO_2$) predicted by GCMs. A similar approach was followed by Mimikou et al. (1991) for the Upper Acheloos and Portaikos rivers in Greece, and by Valdes et al. (1994) in the study of soil moisture and runoff at various sites in the state of Texas, USA. Vaccaro (1993) studied the sensitivity of groundwater recharge to climatic change in the Columbia Plateau, state of Washington, USA. Miller and Russell (1992), simulated annual runoff in 33 of the world's largest river basins under the equilibrium $2 \times CO_2$ scenario. Nash and Gleick (1993) analyzed the sensitivity of streamflow and water supply in the Colorado river basin owing to climatic change. Hostetler and Giorgi (1993) linked a regional climate model (RCM) with a landscape-scale hydrologic model (LSHM) to simulate streamflow in the Steamboat Creek, state of Oregon. Their RCM has a $3000 \times 3000$ km$^2$ domain centered over the Great Basin of the western United States. The RCM, with a

60 km grid spacing, has been calibrated specifically to simulate synoptic-scale weather systems over the mountainous terrain of the western United States. We will focus our analysis of regional hydrologic simulations on the papers by Miller and Russell (1992) and Nash and Gleick (1993). They are representative of some of the limitations and capabilities of regional-scale hydrological simulations over a broad range of geographical areas.

### *6.1. Runoff simulation in large river basins under the equilibrium 2 × $CO_2$ scenario*

Simulations of runoff in a warmer climate are of particular significance in hydrologic studies. The largest water resources systems in the world are dependent on regulated runoff at large reservoirs. Hydrologic models that are nested within GCMs ultimately aim at describing the fate of precipitation once it reaches the surface. Evapotranspiration, soil and groundwater recharge, and runoff are the key components of that analysis (Zektser and Loaiciga, 1993).

In their study of world river runoff, Miller and Russell (1992) used the Goddard Institute for Space Studies (GISS) model described by Hansen et al. (1983) to simulate river runoff for both the present climate ($1 \times CO_2$) and the equilibrium, doubled-$CO_2$ ($2 \times CO_2$), climate. The GISS GCM has a horizontal resolution of 4° latitude by 5° longitude (about $450 \times 550$ km$^2$ cells) and nine vertical layers. The GCM solves numerically the coupled equations for conservation of mass, water vapor, total energy, and momentum, and includes source terms for heat, water vapor, and momentum resulting from processes such as radiation, condensation, and surface interaction. The model predicts precipitation, $P$, among other variables, on the $4° \times 5°$ surface grid cells. The drainage basins for the rivers studied were defined at a horizontal map resolution of $2° \times 2.5°$ (approximately $225 \times 275$ km$^2$ cells). Therefore, each of the $4° \times 5°$ grid cells in the GCM overlaid four of the $2° \times 2.5°$ land grid cells. The GCM's predicted annual runoff was distributed within these $2° \times 2.5°$ cells. The mean annual runoff for a river basin was calculated as the sum of the runoff in each of the $2° \times 2.5°$ cells comprised within the entire river basin. Only rivers with a mean annual runoff larger than 10 km$^3$ were included, resulting in a total of 33 major rivers world-wide.

The hydrology in the GISS model used by Miller and Russell (1992) is rather crude. Evapotranspiration is calculated within the GCM's grid by means of a mass transfer equation that includes the effect of near-surface wind speed, gradient of specific humidity, and soil moisture conditions. Runoff is calculated (in each of the $4° \times 5°$ cells) as the larger of

$$\frac{1}{2}P(W/W_c)$$

or $P + W - W_c$, where $P$ is precipitation predicted by the GISS GCM, $W$ is the water in the top soil layer considered in the model, and $W_c$ is the water field capacity in that soil layer. The rationale behind this empirical runoff equation is that runoff is a fraction of precipitation, and that fraction is determined by the status of soil moisture in the upper soil layer. In the GISS GCM model $W_c > W$, since the water field

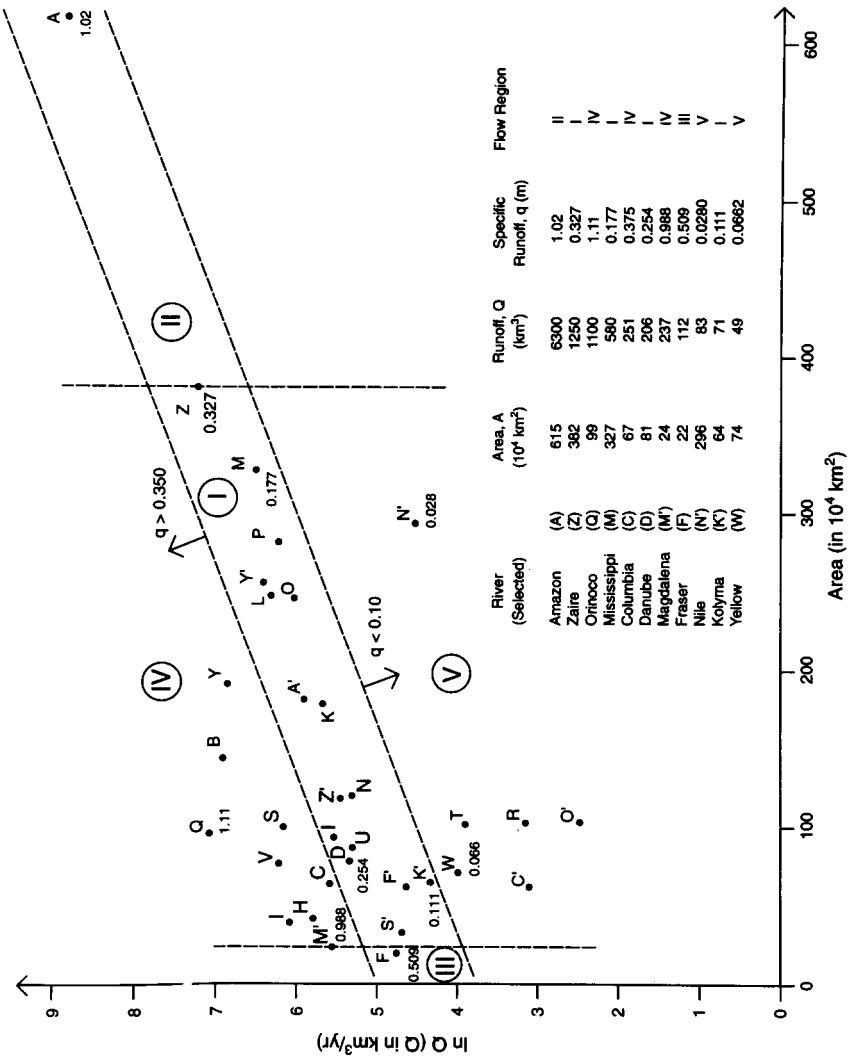


Fig. 15. Representation of mean annual runoff versus area in a semilogarithmic scale for the 33 largest rivers of the world (A, Amazon; B, Brahma-Ganges; C, Columbia; D, Danube; F, Fraser; H, Hsi-Chiang; I, Irrawaddy; K, Mackenzie; L, Lena; M, Mississippi; N, Niger; O, Ob; P, La Plata; Q, Orinoco; S, Saint Lawrence; T, Tigris–Euphrates; U, Yukon; V, Mekong; W, Yellow; Y, Yangtze; Z, Zaire (Congo); A′, Amur; C′, Colorado; F′, San Francisco; I′, Indus; K′, Kolyma; M′, Magdalena; N′, Nile; O′, Orange; R, Murray; S′, Severnaya Dvina; Y′, Yenesei; Z′, Zembesi).

capacity is defined in that model as the soil water content at saturation (as opposed to standard hydrologic jargon where field capacity refers to the volume of water retained in the soil after gravitational water drainage ceases). The water field capacity depends on vegetation characteristics. The half factor appearing in the runoff equation is a 'calibration factor' consistent with observations by Hansen et al. (1983). (Recent modifications of the GISS GCM's surface hydrology parametrization have been reported by Abramopoulos et al. (1988) and by Marengo and Druyan (1994), and Marengo et al. (1994).)

Before discussing the GCM predictions of river basin runoff under the $1 \times CO_2$ and $2 \times CO_2$ scenario by Miller and Russell (1992), let us examine some key features of the relationship, or lack of it, that arises between drainage area and mean annual runoff in the 33 largest rivers of the world. The relationship between runoff and tributary area has received wide attention in hydrology (Strahler, 1958; Rodier and Roche, 1984; Gupta and Waymire, 1990; Smith, 1992). Drainage area is thought to be a factor in the amount of basin runoff; thus, hydrologists have looked thoroughly for consistent laws that might relate them. We have seen that spatial scales are critical in the interfacing of GCMs with hydrologic models. It is natural then to ponder possible connections between measured tributary area (in this example taken from Milliman and Meade, 1983) and measured runoff (United Nations Educational, Scientific, and Cultural Organization (UNESCO), 1985) of the rivers studied by Miller and Russell (1992). Fig. 15 has a plot of the natural logarithm of runoff ($\ln Q$) and tributary area for the 33 river basins with a mean annual runoff in excess of 10 $km^3$. It can be seen that the plot has a great deal of scatter, indicating that area, $A$, is not a good predictor of runoff, $Q$, in this case. A plot of the logarithm of runoff versus the logarithm of area resulted in an equally poor statistical association between mean annual runoff and area. Regressions fit to the model $Q = be^{cA}$, an exponential law with parameters $b$ and $c$, and to the model $Q = bA^c$, were poor, with regression coefficients of less than 25% in both cases. Fig. 15 shows, however, that using a classification of rivers based on specific discharge, $q = Q/A$ (in meters), a different picture of the relationship between runoff and area emerges. Rivers with a specific discharge between 0.10 and 0.35, with two exceptions, the Amazon river (code A in Fig. 15, and the river with the largest tributary area) and the Frazier river (code F in Fig. 15, and the river with the smallest drainage area), follow closely an exponential law relating runoff to area. These rivers are included within regions labeled I, II, and III in the semilog plot of Fig. 15. The exponential relationship between mean annual runoff and area for rivers in regions I, II and III is $Q = 85.422\exp(0.00681A)$, with $Q$ in $km^3$ and area in $10^4$ $km^2$ (the coefficients $b$ and $c$ were estimated by linear regression with a regression coefficient of 0.95). Rivers with a specific discharge larger than 0.35 (flow region IV in Fig. 15), of which the Orinoco (code Q) is the extreme with a $q = 1.11$ m, or rivers with a specific discharge less than 0.10 (flow region V in Fig. 15), the Colorado river of the United (C′) and the Nile river (N′) are examples, defy any sort of statistical association between observed mean annual runoff and observed drainage area.

Table 5 presents a summary of the GCM predicted runoff under the current climate ($1 \times CO_2$) and equilibrium climate for doubled atmospheric carbon dioxide ($2 \times CO_2$). In Table 5, we selected 18 of the 33 rivers under consideration, some of

Table 5
River classification and comparison between observed and GCM-simulated runoff.

| River | Area ($10^4$ km$^2$) | Obs. $Q$ (km$^3$ year$^{-1}$) | $1 \times CO_2$ Q (km$^3$ year$^{-1}$) | $2 \times CO_2$ Q (km$^3$ year$^{-1}$) | Flow region |
|---|---|---|---|---|---|
| Amazon (A) | 615 | 6300 | 2868 | 2958 | II |
| Zaire (Z) | 382 | 1250 | 2166 | 2750 | I |
| Orinoco (Q) | 99 | 1100 | 410 | 802 | IV |
| Brahma-Ganges (B) | 148 | 971 | 1200 | 1186 | IV |
| Yangtze (Y) | 194 | 900 | 1311 | 1782 | IV |
| Mississippi (M) | 327 | 580 | 566[a] | 678 | I |
| Yenesei (Y′) | 258 | 560 | 450[a] | 639 | I |
| Lena (L) | 250 | 514 | 565[a] | 712 | I |
| St. Lawrence (S) | 103 | 447 | 442[a] | 468 | IV |
| Columbia (C) | 67 | 251 | 252[a] | 256 | IV |
| Magdalena (M′) | 24 | 237 | 246[a] | 185 | IV |
| Danube | 81 | 206 | 259 | 308 | I |
| Fraser (F) | 22 | 112 | 115[a] | 125 | III |
| San Francisco (F′) | 64 | 97 | 243 | 225 | I |
| Nile (N′) | 296 | 83 | 624 | 541 | V |
| Yellow (W) | 74 | 49 | 556 | 725 | V |
| Tigris-Euphrates (T) | 105 | 46 | 84 | 81 | V |
| Colorado (C′) | 64 | 20 | 92 | 104 | V |

[a] Rivers for which $1 \times CO_2$ Q is within ±20% of obs. $Q$.

which have a mean annual runoff over 500 km$^3$, others have a mean annual runoff between 500 and 100 km$^3$, and others have a mean annual runoff of less than 100 km$^3$. These rivers in Table 5 encompass all previous flow regions defined in Fig. 15 (I–V). In order to assess the predictive skill of the GISS GCM, observed runoff is compared with the current-climate ($1 \times CO_2$) runoff predicted by the GCM as reported by Miller and Russell (1992). In Table 5 those rivers for which the discrepancy between observed mean annual runoff and current-climate predictions did not exceed ±20% are marked with the superscript 'a'. It is seen that for rivers with a low specific discharge ($q < 0.10$), the GCM predictions for the current climate grossly overestimated mean annual runoff (see, for example, the Nile river). For rivers with a large specific discharge, such as the Amazon ($q = 1.02$) and the Orinoco ($q = 1.11$), the GCM predictions were gross underestimations. The ±20% accurate predictions occurred mostly for rivers in flow region I ($0.10 < q < 0.35$) or rivers close to the boundary between regions I and IV, such as the Saint Lawrence and the Columbia. The Fraser river in region III (where the exponential runoff–area relationship holds) was very accurately predicted. In view of the GCM's poor predictive skill under the current climate, it is pointless to assess the quality of predictions for a $2 \times CO_2$ scenario, although the values reported by Miller and Russell (1992) are presented in Table 5 also. The $2 \times CO_2$ runoff values depart considerably from runoff observations.

This analysis of GCM predicted runoff at regional and continental scales shows

that simplistic representation of the hydrologic cycle within a global model of general atmospheric circulation leads to poor hydrologic predictive skill. In order to model better basin-wide runoff over the entire globe, hydrologic models must be interfaced with GCMs, calibrated, and validated. These models must be suitable to capture the wide-ranging vegetation, physiographic, and climatic characteristics encountered over broad geographical regions. This, as we have seen, is a formidable challenge.

### *6.2. An example of specific basin-wide analysis with water resources impacts*

The second example to be analyzed is that by Nash and Gleick (1993). Unlike the previous example, Nash and Gleick focused on a specific river basin, the Colorado river in the western United States. Fig. 16 depicts the modelling approach followed by Nash and Gleick (1993). Several GCMs (GISS, GFDL, UKMO) were used to simulate climate over the Colorado river for double $CO_2$ conditions. Precipitation and temperature predictions, from both the GCMs as well as from hypothetical scenarios (e.g. percent changes in basin precipitation concurrent with changes in temperature), were then input to the National Weather Service River Forecasting and Simulation (NWSRFS) hydrologic model to simulate the river-basin hydrologic cycle, including runoff. The runoff output originated from the GCMs and hypothetical scenarios were then fed into a water storage and distribution system, the Colorado River Simulation System (CRSS). The CRSS takes runoff inputs throughout the Colorado river basin, routes the runoff, applies reservoir operation rules and diversions to the runoff, and calculates water deliveries, hydropower production, reservoir spills, reservoir storage, and salinity levels at various points throughout a complex net of tributaries, reservoirs, and other water infrastructure that make up the backbone of the Colorado river water supply system. By linking atmospheric,

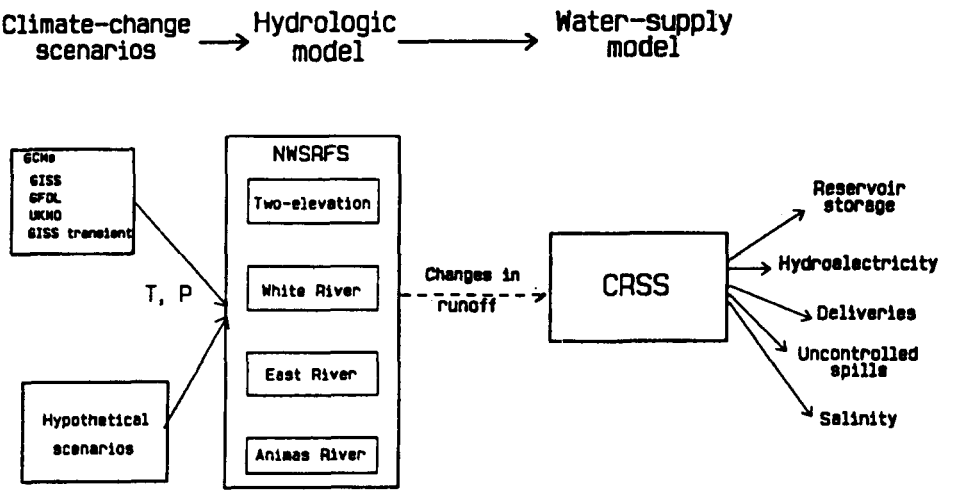


Fig. 16. Modelling system for the Colorado river basin (after Nash and Gleick, 1993).

hydrologic, and river simulation models Nash and Gleick (1993) were able to assess the potential impacts of greenhouse warming in the Colorado river basin.

The entire runoff record for the Colorado river basin was used to calibrate the NWSRFS hydrologic model; therefore, there was no independent validation test as recommended in Table 4. (The differential split-sample test is the appropriate test in this case of transient climatic conditions.) Fig. 17 shows a representative set of results from Nash and Gleick (1993). They considered in this particular instance two scenarios: one where the mean global surface is 2°C warmer, and another with the mean global surface 4°C warmer. For each of these two changed scenarios, precipitation variations ranging from −30% to 30% were considered. The NWSRFS hydrologic model was then simulated to estimate annual runoff for various levels of precipitation. Fig. 17 has the precipitation/runoff relationship so calculated for the White river (a tributary of the Colorado river). For both the 2°C and 4°C temperature changes, the slope of $\Delta Q/\Delta P$ estimated curves in Fig. 16 was nearly 1:1. Therefore, a percent change in precipitation led to a nearly equal percent change in runoff. Other authors (Mimikou et al., 1991) have conducted similar precipitation/runoff studies in relation to climatic change. Mimikou et al. (1991), however, reported an observed 'magnification' effect, whereby, in some basins, the percent change in runoff has exceeded the percent change in precipitation. The reader is referred to Nash and Gleick (1993) for further details of their assessment of water supply impacts of climate change, seasonal hydrologic predictions (the NWSRFS was run with daily time steps), and the like.

Various other studies are found in the literature which examine the hydrologic

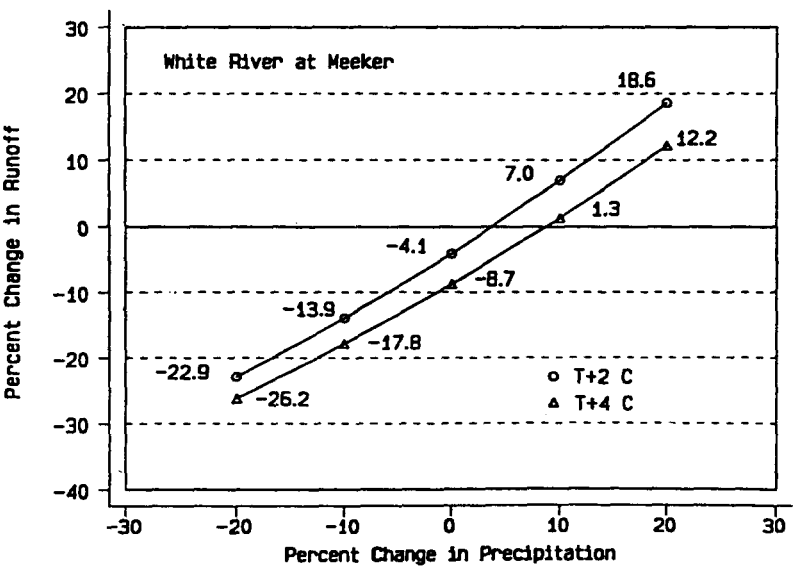


Fig. 17. Relationship between precipitation/runoff changes for different climate scenarios (after Nash and Gleick, 1993).

impact of greenhouse warming. By either setting climate scenarios or simulating the climate with GCMs, climate 'forcings' are input to hydrologic models to simulate runoff at various time and spatial scales. These simulations, typically framed within Monte Carlo simulation schemes, can be conducted to assess hydrologic variability, frequency analysis, etc., under the greenhouse scenario (Rind et al., 1992). The weakest link in assessing hydrologic impacts of climate change remain, however, the models themselves and the difficulty in validating their results. Strictly speaking, without such validation the results reflect only the sensitivity of the model to changes in their parameters, while their correspondence to reality remains in doubt.

## 7. Butterfly effect, global environmental engineering, and other issues

### *7.1. Initial conditions, parameters values, and the butterfly effect*

There are further complications in the study of climate evolution, as well as new ideas about what could be done to stem potential irreversible climatic changes. One important aspect in modeling hydrologic impacts of greenhouse warming is the so-called butterfly effect. This effect is allegorical concerning the chaotic nature of weather, as shown by Lorenz (1963, 1964): if a butterfly were to flap its wings in some part of the world it would disturb the atmosphere around it, thus triggering a divergent weather pattern. This is, of course, an extreme and fabled view of weather and climate sensitivity, let alone hydrologic sensitivity. It has, however, significance to the sensitivity of climate and hydrological change to initial conditions. Tsonis (1991)

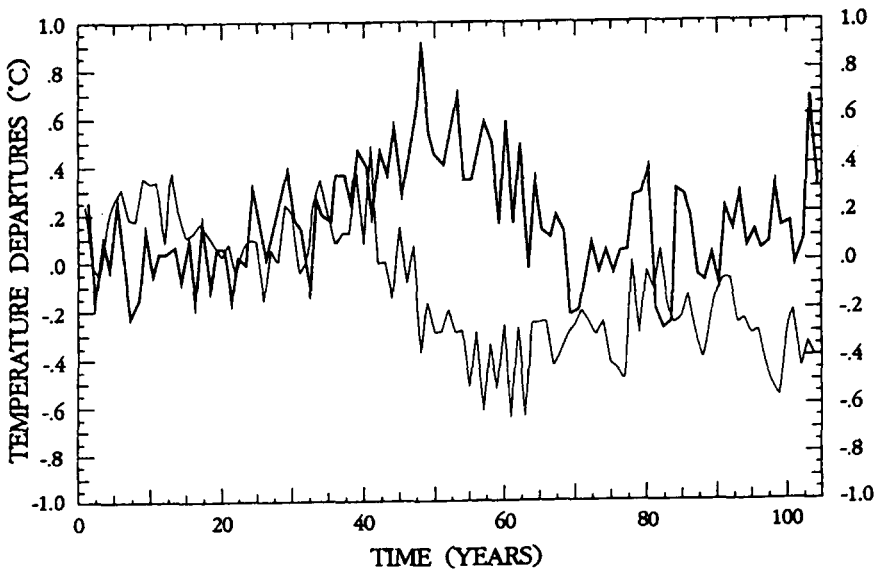


Fig. 18. Behavior of annual global surface mean temperature departures according to Tsonis (1991).

calibrated an autoregressive model to observed global mean surface temperature. Then, he simulated temperature departures from the mean for the next 108 years (extending to year 2100). He did so starting with initial temperature departures that were only 1% apart. Fig. 18 shows how the two simulated temperature records evolved. After 40 years of simulation the two simulated records had no resemblance to each other. The implication here is that if the real climate evolves in a manner somewhat different to what GCMs predict, as it most likely will to some extent, then, some 40 years hence one could expect real and simulated temperature departures from the current mean to diverge in a way resembling Fig. 18. This is assuming a perfectly calibrated GCM. Small variations in model structure, or even in key parameters, also can evoke chaos from fixed initial conditions.

### *7.2. Global environmental engineering*

In view of the uncertainty about the future effects of induced greenhouse warming, some sectors of the scientific community and of the world community at large have called for preventive action (Intergovernmental Panel on Climate Change, 1991). A bolder approach has been suggested by others. The National Academy of Sciences (1991) and Keith and Dowlatabadi (1992), among others, have examined a variety of global environmental engineering options (more appropriate terminology than the alternative 'geoengineering'). Global engineering actions are defined as 'actions taken with the primary goal of engineering (controlling by the application of science) the climate system... it is the deliberate manipulation of climate forcings intended to keep the climate in a desired state, in contrast to abatement which reduces anthropogenic forcing' (Keith and Dowlatabadi, 1991). Some of the actions that have been contemplated are: (1) the launching of solar shields to reflect part of the solar radiation; (2) large-scale reforestation to remove atmospheric $CO_2$; (3) injection of sulfur dioxide ($SO_2$) into the atmosphere to increase its reflectivity and light-scattering properties; (4) direct injection of fossil carbon and $CO_2$ into the oceans, to cite a few. All of these actions have a range of pros and cons, varying costs, uncertainty of effectiveness, and raise equity issues (who bears the costs, who bears negative effects, etc.?). These suggested actions seem unlikely in the foreseeable future, as the launching of international efforts to undertake them appears unrealistic at this time for a variety of scientific reasons, some of which have been examined in this paper, and owing to obvious political and national reasons.

## 8. Implications for water resources engineering

What is the significance of climatic change to the water resources engineer? The answer to this question rests, to some extent, on the previous analysis of greenhouse warming and the hydrologic cycle, and largely on the idiosyncrasies of the water resources engineering profession. There is a substantial body of literature on the policy analysis of climate change in general (not limited exclusively to global

warming) and its impacts on planning, design, and management of the water resource. An early study was conducted by the National Academy of Sciences (1977), which looked into the matter of climate change impacts on water supply in the United States. More recent works on the subject are those by Waggoner and Revelle (1990), US Army Corps of Engineers (1991).

Identifying the practical implications of global warming is an elusive task, as this is an attempt to materialize, in very concrete terms, a rather dubious set of hypotheses, predictions, and scenarios whose consequences might be decades away, if at all. Water resources engineers routinely grapple with issues concerning structural safety, quality of services, regional planning and impacts of water projects, all of which are affected by hydrologic and other uncertainties (Klemes, 1978; Loaiciga and Marino, 1986). Their decisions are based on historical data or projected trends based on observations. Future events, and their uncertainty, are incorporated in water resources decision making, typically by assuming that the future will be a statistical replicate of the hydrologic regime recorded in the past (this is the so-called critical period approach which has been much debated among hydrologists). More sophisticated time-series and stochastic hydrologic analyses are possible when relevant trends are identified in hydrologic records. Future hydrologic uncertainty arising from global warming is of a different nature, however, as that uncertainty is not documented by observation, but rather, is based strictly on climate/hydrologic predictions of limited reliability.

For areas for which detailed studies of the water resources impacts of climate change have been conducted, potential water resources impacts of global warming are generally negative, such as shorter duration of the precipitation season and increase in hydrologic extremes (floods or dry spells). Shorter duration of the precipitation season, possibly coupled with an overall larger annual precipitation and a shift from snow precipitation to rainfall, means larger volumes of runoff generated over shorter time intervals. More runoff would occur in the winter and less runoff would result from spring snowmelt (Lettenmaier and Gan, 1990; Nash and Gleick, 1993). This complicates the storage and routing of floods, both for the purpose of protecting life and property as well as for meeting water supply targets. It also complicates the conjunctive utilization of surface water and groundwater, as the opportunity time for groundwater recharge is reduced under these conditions. The higher incidence of summer dry spells, as predicted by GCMs in continental areas of North America, would reinforce the water-supply problems created by shorter precipitation seasons. In areas where precipitation remains unaffected but mean surface temperatures rise, evapotranspiration is likely to increase at the expense of reductions in streamflow, thus diminishing watershed yields. In tropical latitudes, blessed with relatively even seasonal precipitation, where snowfall is minimal and mean temperatures are relatively high and uniform throughout the year, the water resource is not likely to suffer changes under the previously discussed climate-change scenarios. (Increased hurricane activity in tropical areas under the greenhouse warming scenario has been raised as a possible area of concern. This, however, is an unproven and somewhat far-fetched assertion.)

The other aspect of this discussion on climatic change and water resources

engineering is the water resources engineering profession itself. Water resources infrastructure design and planning, just like any other type of civil project, are inherently conservative. By this it is meant that, given the uncontrollable uncertainty found in natural phenomena and people's behavior, sound engineering designs and plans are conceived to err on the safe side. This is what one might call the 'safety-first principle' of engineering practice, conspicuous in the 'safety factor' of structural design or in the Probable Maximum Precipitation (PMP) of flood-control design, for example. The concern for safety and social welfare in water resources engineering explains, as shown by Loaiciga and Marino (1986), why water projects of regional, macroeconomic scope in open societies are not implemented to maximize economic efficiency criteria, but rather, to maximize a social utility function that is intrinsically risk-averse.

It has been stated earlier in this work that the natural variability in regional hydrologic cycles is likely to dominate additional variability brought about by climate change. Sound water resources engineering, with its provisions for safety as they now stand, ought to render water projects adequate with or without climate change. Klemes (1991) has put forward a series of specific guidelines to cope with future climate change contingencies in the context of water resources engineering practice: (1) adherence to high professional standards in proposing solutions to existing water resource problems, (2) commitment to measures limiting water waste and pollution, (3) striving for robust and resilient designs, (4) documenting and taking into account known uncertainties in water supply and demand, (5) documenting the ranges of feasible operation of projects, rather than providing only nominal design parameters, (6) providing a general outline of feasible contingency measures for extreme conditions not accommodated by the project under normal operation (i.e. flexible operating rules), and (7) insistence on clear disclosure of factual information, assumptions, and conjectures behind modeling results to be considered.

## 9. Summary and conclusions

The potential rapid warming of the Earth induced by greenhouse gases has triggered a storm of scientific inquiry and a frenzy of political posturing. The processes of climate evolution, hydrologic regime modification, and, in general, environmental (as well as socioeconomic) impacts are the subject of intense argument and study. For the hydrologist and water planner, the issues at stake are possible modifications of hydrologic regimes at the scale of the river basin. This scale, as we have seen, can vary from tens of kilometers to thousands of kilometers.

Starting with a review of the basic processes that govern greenhouse warming, we have demonstrated that the hydrologic cycle plays a key role in the heat balance of the atmosphere. Through the water feedback, the hydrologic cycle is bound to have a central role in the climate's evolution as greenhouse gases continue to build up in the atmosphere. This guided tour of the hydrologic cycle's role in the greenhouse phenomenon, past, present, and future, has highlighted the roles of many other feedbacks on the climate that are likely to intensify if induced greenhouse warming

sets in as predicted. Furthermore, climate feedbacks will interact with each other, rendering the climate's evolution a rather complicated process.

Areas that have been identified as deserving continued attention and further research are: (1) ocean–atmosphere coupling, (2) vegetation and evapotranspiration (land–atmosphere interactions, in general), (3) climate feedbacks, (4) global data sets on large-scale dynamics, and (5) validation of models, hydrologic and otherwise (see Dooge, 1992, for an expanded analysis of this last item). In other words, the entire process of data collection, their analysis, development of knowledge about climate/hydrology dynamics under greenhouse warming, and translation of this knowledge into models with realistic predictive skills, needs continued support and attention to rigor.

General circulation models, the only available tool for detailed modeling of future climate evolution, are not well suited for answering the questions of primary interest to hydrologists concerning regional-scale hydrologic variability. GCMs were not developed for that purpose. They were originally developed to predict the average, synoptic-scale, general-circulation patterns of the atmosphere. Embedding schemes linking GCMs to meteorologic and hydrologic models resolved at finer scales have been proposed and implemented. This is the state-of-the-art approach to bridge the gap between the coarse-resolution GCMs and hydroclimatic modelling at the river-basin scale. In addition, water storage and distribution models have been interfaced with the hydrologic models to assess the sensitivity of water resources systems to climatic change. GCMs simulate the climate at the synoptic scale or the mesoscale. Their predictions act as boundary and initial conditions to the finer-resolution meteorological, hydrological, and river simulation models nested within them. Provided that CGM simulations of the climate are accurate under the greenhouse warming scenario and that the hydrologic models are also accurate, one has, then, a way to assess hydrologic regimes in a warmer climate.

The reality, however, is that GCMs are not accurate predictors of climate evolution caused by rising concentrations of greenhouse gases. Moreover, hydrologic models embedded within GCMs to simulate the hydrologic cycle are difficult to calibrate, and, literally, impossible to validate given the absence of adequate spatial and temporal data applicable to a warming planet. In spite of these shortcomings, the hydrologic literature now abounds with regional-scale hydrologic simulations under greenhouse scenarios. Such scenarios are either GCM-simulated or hypothetical. In the midlatitudes, these hydrologic simulations typically point to shorter winter seasons, larger floods, rising snow lines in mountainous areas, drier summer spells, and, in general, to more pronounced and protracted cycles of hydrologic variability. At the global scale, GCM simulations predict an intensified hydrologic cycle, with greater evapotranspiration and precipitation overall.

As for the policy and water resources engineering implications of potential global warming, it is our opinion that sound exercise of water resources engineering principles and standards as they now stand ought to be adequate to deal with additional hydrologic uncertainty that might arise from global warming. Commitment to averting water waste and pollution, robust and resilient designs, flexible operational policy, accounting for extreme conditions that might arise, prioritization of public

safety, and exercise of educated professional judgement substantiated with the best documented information available, are the guidelines for practising water resources engineering with or without climate change.

It seems prudent for hydrologists to pursue their contributions to the scientific and policy issues of global warming, however limited these might be. The debate surrounding greenhouse warming is not going to abate in the foreseeable future. Important policy decisions could be forthcoming as a result that will affect the water institutions in this and other countries. They might as well be informed ones.

## Acknowledgments

This work was made possible by the support of the American Society of Civil Engineers for the Task Committee on Global Warming and Hydrological Variability, whose members have written this paper. The first author also acknowledges the support of the National Science Foundation through grant NSF-SES-88-109-17 to the National Center for Geographic Information and Analysis of the Department of Geography at UC Santa Barbara, and of the Kearney Foundation through grant 92-09. Dr. V. Klemes contributed reference materials and valuable suggestions on the implications of global warming on water resources engineering. Dr. N. Fennessey suggested important references and made helpful clarifications concerning the contents of this work.

## References

Abramopoulos, F., Rosenzweig, C. and Choudhuri, B., 1988. Improved ground hydrology calculations for global climate models (GCMs): soil water movement and evapotranspiration. J. Climate, 1: 921–941.

Ahrens, C.D., 1994. Meteorology Today, 5th edn. West Publishing, Minneapolis, MN.

Amorocho, J. and Espildora, B., 1973. Entropy in the assessment of uncertainty in hydrologic systems and models. Water Resour. Res., 9: 1511–1522.

Arrhenius, S., 1896. On the influence of carbonic acid in the air on the temperature on the ground. Philos. Mag., 41: 237–276.

Avissar, R. and Verstraeter, M. M., 1990. The representation of continental surface processes in atmospheric models. Rev. Geophys., 28: 35–52.

Barros, A.P. and Lettenmaier, D.P., 1993. Multiscale aggregation and disaggregation of precipitation for regional hydroclimatological studies. In: W.B. Wilkinson (Editor), Macroscale Modelling of the Hydrosphere, Proc. of the Yokohama Symp., Yokohama, 21–25 July. IAHS Publ. No. 214, IAHS, Wallingford, pp. 183–193.

Briffa, K.R., Bartholin, T.S., Eckstein, D., Jones, P.D., Karlen, W., Schweingruber, F.H. and Zetterberg, P., 1990. 1400-year tree-ring record of summer temperatures in Fennoscandia. Nature, 346: 434–439.

Cess, R.D., et al., 1990. Intercomparison and interpretation of climate feedback processes in 19 general circulation models. J. Geophys. Res., 95: 16601–16615.

Chamberlin, T.C., 1897. A group of hypothesis bearing on climatic change. J. Geol., 5: 563–568.

Del Genio, A.D., 1993. Convective and large-scale cloud processes in GCMs. In: E. Raschke and D. Jacob (Editors), Energy and Water Cycles in the Climate System. NATO ASI Series I, Vol. 5, Springer, Berlin, pp. 95–121.

Dickinson, R.E., 1989. Implications of tropical deforestation for climate: a comparison of model and observation and description of surface energy and hydrological balance. Philos. Trans. R. Soc. London, Ser. B, 324: 423–431.

Dickinson, R.E. and Henderson-Sellers, A., 1988. Modelling tropical deforestation: a study of a GCM land-surface parameterization. Q. J. R. Meteorol. Soc., 114: 439–462.

Dickinson, R.E., Henderson-Sellers, A., Kennedy, P.J. and Wilson, M.F., 1986. Biosphere–atmosphere Transfer Schemes (BATS) for the NCAR Community Climate Model. In: NCAR Technical Note NCAR/TN-275+STR, National Center for Atmospheric Research, Boulder, CO.

Dooge. J.C.I., 1992. Hydrologic models and climate change. J. Geophys. Res., 97(D3): 2677–2686.

Eagleson, P.S., 1991. Hydrologic science: a distinct geoscience. Rev. Geophys., 29(2): 237–248.

Entekabi, S. and Eagleson, P.S., 1989. Land-surface hydrology parameterization for atmosphere general circulation models including subgrid-scale spatial variability. J. Climate, 2: 816–831.

Giorgi, F. and Mearns, L.O., 1991. Approaches to the simulation of regional climate change — a review. Rev. Geophys., 29: 191–216.

Gleick, P.H., 1986. Methods for evaluating the regional hydrologic impacts of global climatic changes. J. Hydrol., 88: 99–116.

Gleick, P.H., 1987. Regional consequences of increases in atmospheric $CO_2$ and other trace gases. Climate Change, 10: 137–161.

Goodwin, I., 1994. Counting what counts: 1995 budget skips science, boots technology. Phys. Today, April: 49–55.

Graedel, T.E and Crutzen, P.J., 1993. Atmospheric Change. W.H. Freeman and Co., New York.

Gupta, V. and Waymire, E., Multiscaling properties of spatial rainfall and river flow distribution. J. Geophys. Res., 95(D3): 1999–2010.

Hansen, J., Russel, G., Rind, D., Stone, P., Lacis, S., Lebedeff, S., Ruedy, R. and Travis, L., 1983. Efficient three-dimensional global models for climate studies; models I and II. Mon. Weather Rev., III: 609–662.

Harrison, E.F., Mianis, P., Barkstrom, B.R., Ramanathan, V., Cess, R.D. and Gibson, G.G., 1990. Seasonal variation of cloud radiative forcing derived from the earth radiation budget experiment. J. Geophys. Res., 95: 18 681–18 703.

Holton, J.R., 1992. An Introduction to Dynamic Meteorology, 3rd edn. Academic, San Diego, CA.

Hostetler, S.W. and Giorgi, F., 1993. Use of output from high-resolution atmospheric models in landscape-scale hydrologic models: an assessment. Water Resour. Res., 29: 1685–1695.

Intergovernmental Panel on Climate Change (IPCC), 1990. Climate Change, The IPCC Scientific Assessment. J.T. Houghton, G.J. Jenkins and J.J. Ephraums (Editors). Cambridge University, Cambridge.

Intergovernmental Panel on Climate Change (IPCC), 1991. Climate Change, The IPCC Response Strategies. Island, Washington, DC.

Karl, T.R., Hein, R.R. and Quayle, R.G., 1991. The greenhouse effect in North America: if not now, when? Science, 251: 1058–1061.

Keith, D.W. and Dowlatabadi, A., 1992. A serious look at geoengineering. EOS, Trans. Am. Geophys. Union, 73: 289–293.

Klemes, V., 1978. The unreliability of reliability estimates of storage reservoir performance based on short streamflow records. In: Reliability in Water Resources Management. Water Resources, Fort Collins, CO, pp. 193–205.

Klemes, V., 1985. Sensitivities of water resources systems to climate variations. Rep. No. WCP-98, World Climate Program, World Meteorological Organization, Geneva.

Klemes, V., 1986. Operational testing of hydrological simulation. Hydrol. Sci., 31(1): 13–24.

Klemes, V., 1991. Design implications of climate change. In: T. Ballentine and E.Z. Stakhiv (Editors), Proc. First National Conf. of Climate Change and Water Resources, United States Army Corps of Engineers, Washington, DC, pp. III-9–III-19.

Lawford, R.G., 1993. The role of ice in the global water cycle. In: W.B. Wilkinson (Editor), Macroscale Modelling of the Hydrosphere, Proc. Yokohama Symp., Yokohama, 21–25 July. IAHS Publ. No. 214, IAHS, Wallingford, UK, pp. 151–161.

Lettenmaier, D.P. and Gan, T.Y., 1990. Hydrologic sensitivities of the Sacramento–San Joaquin river basin, California, to global warming. Water Resour. Res., 26: 69–86.

Lindzen, R.S., 1990. Some coolness concerning global warming. Bull. Am. Meteorol. Soc., 71: 288–299.

Lins, H.F. and Michaels, P.J., 1994. Increasing streamflow in the United States. EOS, Trans. Am. Geophys. Union, 75(25): 281, 284–285.

Loaiciga, H.A. and Marino, M.A., 1986. Risk analysis for reservoir operation. Water Resour. Res., 22(4): 483–488.

Loaiciga, H.A., Haston, L. and Michaelsen, J., 1993. Dendrohydrology and long-term hydrologic phenomena. Rev. Geophys. 31: 151–171.

Lorenz, E.N., 1963. Deterministic non-periodic flow. J. Atmos. Sci., 20: 130–141.

Lorenz, E.N., 1964. The problem of deducing the climate from the governing equations. Tellus, 16: 1–11.

Lvovitch, M.I., 1973. The global water balance. EOS, Trans. Am. Geophys. Union, 54: 28–42.

Manabe, S., 1969. Climate of the ocean circulation, Part I. Mon. Weather Rev., 97: 739–774.

Manabe, S. and Wetherald, R.T., 1987. Large-scale changes in soil wetness induced by an increase in carbon-dioxide. J. Atmos. Sci., 44: 1211–1235.

Manabe, S., Smagorinsky, J. and Strickler, R.F., 1965. Simulated climatology of a general circulation model with a hydrologic cycle. Mon. Weather Rev., 93: 769–798.

Marengo, J.A. and Druyan, M., 1994. Validation of model improvements for the GISS GCM. Climate Dyn., 10: 163–179.

Marengo, J.A., Miller, J.R., Russel, J.R., Rosenzweig, C.E. and Abramopoulos, F., Calculations of river runoff in the GISS-GCM: input of a new land-surface parameterization and runoff routing model on the hydrology of the Amazon river. Climate Dyn., 10: 349–361.

Miller, R. and Russell, G.K., 1992.The impact of global warming on river runoff. J. Geophys. Res., 97(D3): 2757–2764.

Milliman, J.D. and Meale, R.H., 1983. World-wide delivery of river sediment to the oceans. J. Geol., 91: 1–21.

Mimikou, M., Kouvopoulos, Y., Cavadias, G. and Vayianov, N., 1991. Regional hydrologic effects of climate change. J. Hydrol., 123: 119–146.

Mitchell, J.B.F., 1989. The 'greenhouse effect' and climate. Rev. Geophys., 27: 115–139.

Mitchell, J.F.B., Manabe, S., Meleshko, V. and Tokioka, T., 1990. Equilibrium climate change — and its implications for the future. In: J.T. Houghton, G.T. Jenkins and J.J. Ephraums (Editors), Climate Change, The IPCC Scientific Assessment. Cambridge University, Cambridge, pp. 131–172.

Monteith, J.L., 1973. Principles of Environmental Physics. American Elsevier, New York.

Nash, L. and Gleick, P., 1993. The Colorado river basin and climatic change. Rep. EPA 230-R-93-009, United States Environmental Protection Agency, Washington, DC.

National Academy of Sciences, 1977. Climate, Climate Change, and Water Supply. National Academy, Washington, DC.

National Research Council, 1991. Opportunities in the Hydrologic Sciences. National Research Council, Washington, DC.

Oki, K.M., Masuda, K. and Matsuyama, M., 1993. Global runoff estimation by atmospheric water balance using the ECMWF data set. In: W.B. Wilkinson (Editor). Macroscale Modelling of the Atmosphere, Proc. of the Yokohama Symp. IAHS Publ. No. 214, IAHS, Wallingford, UK, pp. 163–171.

Peixoto, J.P. and Oort, A.H., 1992. Physics of Climate. American Institute of Physics, New York.

Phillips, N.A., 1956. The general circulation of the atmosphere: a numerical experiment. Q. J. R. Meteorol. Soc., 82: 123–164.

Ramanathan, V., 1988. The greenhouse theory of climate change: a test by an inadvertent global experiment. Science, 240: 293–299.

Ramanathan, V. and Collins, W., 1991. Thermodynamic regulation of ocean warming by cirrus clouds deduced from observations of the 1987 El Niño. Nature, 351: 27–32.

Ramanathan, V. and Collins, W., 1992. Thermostat and global warming. Nature, 357: 649–653.

Ramanathan, V., Barkstrom, B.R. and Harrison E.F., 1989. Climate and the earth's radiation budget. Phys. Today, May: 22–32.

Ramanathan, V., Cess, R.D., Harrison, H.F., Minnis, P. and Barkstrom, B.R., 1989. Cloud radiative forcing and climate results from the Earth Radiation Budget Experiment. Science, 243: 57–63.

Raschke, E., 1993. Radiation–cloud-climate interaction. In: E. Raschke and D. Jacob (Editors). Energy and Water Cycles in the Climate System. NATO ASI Series I, Vol. 5, Springer, Berlin, pp. 69–93.

Richardson, L.F., 1922. Weather Prediction by Numerical Processes. Cambridge University, London.

Rind, D., Rosenzweig, C. and Goldberg., R., 1992. Modelling the hydrologic cycle in assessment of climate change. Nature, 358: 119–122.

Rodier, J.P. and Roche, M., 1984. World catalogue of maximum observed floods. IAHS Publ. No. 143, Wallingford, UK.

Schlesinger, M.E. and Jiang, X., 1991. Revised projection of future greenhouse warming. Nature, 350: 219–221.

Sellers, P.J., Mintz, Y., Sud, Y.C. and Dalcher, A., 1986. A Simple Biosphere (SiB) for use within general circulation models. J. Atmos. Sci., 43: 505–531.

Sellers, P.J., Shuttleworth, W.J., Dorman, J.L., Dalcher, A. and Roberts, J.M., 1989. Calibrating the simple biosphere model for Amazonian tropical forest using field and remote sensing data, Part I; average calibration with field and remote sensing data. J. Appl. Meteorol., 28: 727–759.

Shine, K.P., Derwent, R.G., Wuebbles, D.J. and Morcrette, J.J., 1990. Radiative forcing of the climate. In J.T. Houghton, G.J. Jenkins and J.J. Ephraums (Editors), Climate Change, The IPCC Scientific Assessment. Cambridge University, Cambridge, pp. 45–68.

Shuttleworth, W.J., 1988. Macrohydrology, the new challenge for process hydrology. J. Hydrol., 100: 31–56.

Shuttleworth, W.J., 1993. The soil–vegetation–atmosphere interface. In: E. Raschke and D. Jacob (Editors), Energy and Water Cycles in the Climate System. NATO ASI Series I, Vol. 5, Springer, Berlin, pp. 323–364.

Smith, J.A., 1992. Representation of basin scale in flood peak distribution. Water Resour. Res., 28: 2993–2999.

Strahler, A., 1958. Dimensional analysis applied to fluvially eroded land forms. Bull. Geol. Soc. Am., 69: 279–300.

Swart, P.K., Lohman, F.C., Mackenzie, J. and Savin, S. (Editors), 1993. Climate Change in Geophysical Continental Isotopic Records. Monogr. No. 78, Am. Geophys. Union, Washington, DC.

Toggweiler, J.R., 1994. The oceans's overturning circulation. Phys. Today, November: 45–50.

Tsonis, A., 1991. Sensitivity of the global climate system to initial conditions. EOS, Trans. Am. Geophys. Union, 72: 313, 328.

United Nations Educational, Scientific, and Cultural Organization (UNESCO), 1985. Discharge of Selected Rivers of the World, Vol. 3, Part 4. UNESCO, Paris.

United States Army Corps of Engineers, 1991. Climate Change and U.S. Water Resources. National Academy Press, Washington, DC.

Valdes, J.B., Seoane, R.S. and North, G.R., 1994. A methodology for the evaluation of global warming impact on soil moisture and runoff. J. Hydrol., 161: 161–389.

Vaccaro, J.J., 1993. Sensitivity of groundwater recharge estimates to climate variability and change, Columbia Plateau, Washington. J. Geophys. Res., 97: 2821–2833.

Vorosmarty, C.J., Gutowsky, W.J., Person, M., Chen, T.C. and Chase, D., 1993. Linked atmosphere–hydrology models at the macroscale. In: W.B. Wilkinson (Editor), Macroscale Modelling of the Atmosphere, Proc. of the Yokohama Symp. IASH Publ. No. 214, IAHS, Wallingford, UK, pp. 3–27.

Waggoner, P.E. and Revelle, R.R. (Editors), 1990. Climate and Water: Climatic Variability, Climate change, and the Planning and Management of the U.S. Water Resources. John Wiley and Sons, New York.

Washington, W.M. and Meehl, G.A., 1989. Climate sensitivity due to increased $CO_2$: experiments with a coupled atmosphere and ocean circulation model. Climate Dyn., 4: 1–38.

Weatherald, R.T. and Manabe, S., 1988. Cloud feedback processes in a general circulation model. J. Atmos. Sci., 45: 1397–1415.

Willebrand, J., 1993. Forcing of the ocean by heat and freshwater fluxes. In: E. Raschke and D. Jacob

(Editors). Energy and Water Cycles in the Climate System. NATO ASI Series I, Vol. 5, Springer, Berlin, pp. 215–233.

Wood, E.F. (Editor), 1991. Land Surface–atmosphere Interactions for Climate Modeling. Kluwer Academic, Dordrecht.

Wood, E.F., Lettenmaier, D.P. and Zartarian, G.P., 1992. A land-surface hydrology parameterization with subgrid variability for general circulation models. J. Geophys. Res., 97(D3): 2717–2728.

Zektser, I.S. and Loaiciga, H.A., 1993. Groundwater fluxes in the global hydrologic cycle: past, present, and future. J. Hydrol., 144: 405–427.